# EFFECT OF NON-SYNCHRONOUS ROTATION* ON CLOSE BINARY STARS



SU-SHU HUANG†

The effect of non-synchronous rotation of the component star in close binaries on its limiting surface is analyzed and the difficulties in the previous investigations are examined. It has been shown that no potential function exists in a coordinate system following the axial (non-synchronous) rotation of the component star. Consequently, no equilibrium surfaces can be obtained in this way. It is therefore suggested that we should retain the conventional coordinate system that rotates with the binary motion. Since a simple energy integral exists in this coordinate system, we can obtain a physical picture for the problem of the non-synchronously rotating star in the binary systems. Indeed we have found that the non-synchronously rotating star will modify its rotation gradually and become eventually synchronous with its orbital revolution.

In this multifarious activities and achievements that make him one of the greatest astronomers in the modern time, Professor Otto Struve has never forsaken the binary stars. After having spent some years of successful researches in other fields of astronomy now and then he always returned to this field of his early interest. Therefore, few astronomers have observed spectroscopically as many binary stars as he has done. Fewer still have left such a distinct mark as his in the history of double stars.

In a close association and collaboration with him for a decade during which I am proud to have received his confidence and learned the process of his mental perceptions and responses as a result of our daily afternoon meetings in cafes outside the North Gate of the Berkeley Campus of the University of California, I have always been impressed by his open mindedness to new ideas, his enthusiasm for and devotions to astronomy. Because of his open mindedness he saw any problem in its multi-faceted angles, thus making him not only an outstanding scientist but also a great leader. Because of his enthusiasm, he enlisted many astronomers into the fields of his interest. Our daily contact also induced me to become a novice in the study of binary stars in the mid fifties: It is therefore befitting for me ten years later to write this article on binary stars in this memorial volume as my attribute to a great leader as well as a dear friend whom I have both respected and admired.

## I. A CRITICAL REVIEW OF THE PREVIOUS INVESTIGATIONS

The shape of stellar surfaces in the close binary system has been given as a first approximation by what has been predicted by the Roche Model (e.g. Struve and Huang 1957. According to this model, the axial rotation of component stars and their orbital revolution are synchronized. While the majority of close binaries indeed obey the rule of synchronization (Swings 1936, Struve 1950, Plaut 1959) there are some exceptions to which belongs $\beta$ Lyrae—a peculiar binary system that Professor Struve (1941, 1958) had a life-long interest. Therefore, in recent years attempts have been made to predict the stellar surfaces, especially the limiting surface, when the component star does not rotate in synchronization with its orbital revolution (Kopal 1956, Plavec 1958, Kruszewski 1963, and Limber 1963).

In the restricted three-body problem one can define a potential function $U$ in a coordinate system that rotates with the binary's orbital motion

*Prepared for a Memorial Volume for Prof. Otto Struve.

†Goddard Space Flight Center and Catholic University, Washington, D. C.

(e.g., Moulton 1914). Also an energy integral can be obtained in the form that the sum of the potential energy and the kinetic energy is constant. It is the existance of the energy integral in this form that enables us to predict the stellar surfaces of close binaries because only then the density and the pressure should be constant on any equi-potential surface. Thus, we should emphasize that the mere existence of a potential function does not necessarily warrant a prediction of the equilibrium surface of a star. Indeed, this is the reason that the calculations by previous investigators have to be regarded as unsatisfactory.

Kopal (1956) first studied the limiting surface of the non-synchronously rotating star, using a potential function which Kruszewski (1963) has since pointed out to be incorrect. Later Plavec (1958), Kruszewski (1963) and Limber (1963) have all derived a potential function and obtained the limiting surface. However, even though their potential function is correct, their result is still open to debate as we may see in the following way.

Let us first choose a dimensionless system of units of measurement with the total mass of the binary as the unit of mass, with the separation between the two components as the unit of length and with $P/2\pi$ as the unit of time, where $P$ stands for the orbital period. Thus, if we denote $1-\mu$ as the mass of one component, $\mu$ will be the mass of the other. Let us further choose a rotating $(x,y,z)$ system such that the origin is at the center of the $1-\mu$ component, the $x$-axis points always towards the $\mu$ component, and the $xy$ plane coincides with the orbital plane. We have the equations of motion for a test particle in the $(x,y,z)$ system:

$$\frac{d^2x}{dt^2}-2\frac{dy}{dt}=\frac{\partial U_1}{\partial x},\quad \frac{d^2y}{dt^2}+2\frac{dx}{dt}=\frac{\partial U_1}{\partial y},\quad \frac{d^2z}{dt^2}=\frac{\partial U_1}{\partial z}, \tag{1}$$

where

$$U_1(x,y,z)\equiv\frac{1}{2}[(x-\mu)^2+y^2]+\frac{1-\mu}{r_1}+\frac{\mu}{r_2} \tag{2}$$

and $r_1$ and $r_2$ are respectively the distances of the test particles from the two component stars. Note that $U_1$ is a function of time only through the coordinates $(x,y,z)$ of the test particle.

We now introduce a new rotating $(\xi,\eta,\zeta)$ system such that it is rigidly fixed to the $1-\mu$ component, sharing the latter's axial rotation. Although the axial rotation of the $1-\mu$ component is not synchronous with the orbital motion, its rotating axis (chosen as the $\zeta$-axis) is still assumed to be perpendicular to the orbital plane. Thus, if the $(\xi,\eta,\zeta)$ system is rotating with an angular velocity, $\omega$, with respect to the $(x,y,z)$ system, it rotates with an angular velocity, $1+\omega$, with respect to the rest frame of reference. The transformation equations between $(x,y,z)$ and $(\xi,\eta,\zeta)$ are as follows:

$$x=\xi\cos\omega t-\eta\sin\omega t,$$
$$y=\xi\sin\omega t+\eta\cos\omega t,\ z=\zeta \tag{3}$$

The equations of motion in the $(\xi,\eta,\zeta)$ system are

$$\frac{d^2\xi}{dt^2}-2(\omega+1)\frac{d\eta}{dt}=-\mu\cos\omega t+\frac{\partial U_2}{\partial\xi} \tag{4}$$

$$\frac{d^2\eta}{dt^2}+2(\omega+1)\frac{d\xi}{dt}=\mu\sin\omega t+\frac{\partial U_2}{\partial\eta} \tag{5}$$

$$\frac{d^2\zeta}{dt^2}=\frac{\partial U^2}{\partial\zeta} \tag{6}$$

where

$$U_2(\xi,\eta,\zeta)\equiv\frac{1}{2}(\omega+1)^2(\xi^2+\eta^2)+\frac{1-\mu}{r_1}+\frac{\mu}{r_2} \tag{7}$$

may be regarded as the negative value of the potential function. Acutally, it is a misleading name as we shall see presently.

$U_2(\xi,\eta,\zeta)$ as given by equation (7) does not give the limiting surface of the non-synchronous $1-\mu$ component. In the first place, we encounter the time-dependent terms $\mu\cos\omega t$ and $\mu\sin\omega t$ in equations (4) and (5). Secondly $r_2$, which is given by

$$r_2^2=(\xi-\cos\omega t)^2+(\eta+\sin\omega t)^2+\zeta^2, \tag{8}$$

is now an explicit function of time. Therefore $U_2(\xi,\eta,\zeta)$, unlike $U_1$ in the $(x,y,z)$ system, is no longer an implicit function of time through the space coordinates alone but involves time explicitly. For brevity we write $U_2(t)$ for $U_2(\xi,\eta,\zeta)$. Because of the two complications, we can no longer derive from equations (4)–(6) the simple result that the sum of the potential energy and the kinetic energy is a constant of motion. Consequently, the surfaces defined by equation (7) do not represent equilibrium surfaces of the star. We can see this point analytically in the following way.

Multiplying equations (4)–(6) respectively by $d\xi/dt$, $d\eta/dt$ and $d\zeta/dt$ and adding the resulting equations together, we obtain after integration with respect to time that

$$\frac{1}{2}[V^2(t)-V^2(t_o)]-[U_2(t)-U_2(t_o)]$$
$$=\int_{t_o}^{t}\left[\mu\left(\frac{d\eta}{dt}\sin\omega t-\frac{d\xi}{dt}\cos\omega t\right)-\frac{\partial U_2}{\partial t}\right]dt, \qquad (9)$$

where $V(t)$ and $V(t_o)$ denote respectively the velocity of the test particle at time $t$ and at the initial time $t_o$. $\partial U_2/\partial t$ may be evaluated from equations (7) and (8). When the result is substituted into equation (9), we obtain finally

$$\frac{1}{2}[V^2(t)-V^2(t_o)]-[U_2(t)-U_2(t_o)]$$
$$=\mu\int_{t_o}^{t}\left[\left(\frac{d\eta}{dt}-\frac{\omega\xi}{r_2^3}\right)\sin\omega t-\left(\frac{d\xi}{dt}+\frac{\omega\eta}{r_2^3}\right)\cos\omega t\right]dt. \qquad (10)$$

It is obvious from equation (10) that the sum of the potential and kinetic energy is no longer constant. Since the integral in equation (10) actually depends upon the path of the test particle, $-U_2$ does not behave exactly like a potential.

The previous investigators have introduced

$$U_3(\xi,\eta,\zeta)=U_2(\xi,\eta,\zeta)+\mu(\eta\sin\omega t-\xi\cos\omega t). \qquad (11)$$

In doing so, they can replace the right hand sides of equations (4)–(6) respectively by $\partial U_3/\partial\xi$, $\partial U_3/\partial\eta$, and $\partial U_3/\partial\zeta$. Because of the transformation relation (3), $U_3(\xi,\eta,\zeta)$ can now be expressed in terms of $x$, $y$ and $z$. In this new expression for $U_3$, time appears only implicitly through $x,y,z$ but does not enter explicity. Consequently, they have independently derived the limiting surface in the $(x,y,z)$ system by considering $U_3$ as the potential function.

However, we should remember that it is the $(\xi,\eta,\zeta)$ system that is rigidly fixed to the rotating star. Any stationary surface of the non-synchronous rotating star ($1-\mu$ component) must be expressed as a function of $\xi$, $\eta$ and $\zeta$ alone without the explicit appearance of time. It does not appear that an expression in $x$, $y$, and $z$ can represent the stationary surfaces of the non-synchronous component because in the $(x,y,z)$ system the component has a net rotation. Since, as we have seen before, we cannot obtain a potential function in the $(\xi\eta,\zeta)$ system, we have no means to compute the stationary surfaces of a non-synchronous rotating component star, a conclusion contrary to the previous investigators.

## II. PHYSICAL INTERPRETATION

Because of the difficulties we have just observed, it is advisable to retain the $(x,y,z)$ coordinate system that rotates with the binary motion. In this coordinate system we have for the test particle a simple energy integral

$$2U_1-V^2=C \qquad (12)$$

where $U_1(x,y,z)$ is given by equation (2).

We should now recall that the zero-velocity surfaces are labelled by $C$ (e.g., Moulton 1914). Let the $C$ value that is associated with the innermost contact surface $S_1$ (Kuiper 1941) be $C_1$. Therefore, all particles inside the $S_1$ surface with $C<C_1$ could penetrate the $S_1$ surface. As a result, these particles will gradually be lost from the star. Now the $1-\mu$ component is rotating with an angular velocity $\omega$ in the $x,y,z$ coordinate system along the $z$-axis. Particles in the stellar surface layers have velocities

$$V=(x^2+y^2)^{\frac{1}{2}}\omega \qquad (13)$$

if thermal motion or other kinds of motion are neglected. Hence, all particles in the $1-\mu$ component star that are above the surface (called the $R$ surface hereafter) given by

$$2U(x,y,z)-\omega^2(x^2+y^2)=C_1 \qquad (14)$$

and consequently have $C$ values less than $C_1$ may be regarded as unstable and could easily escape out of the $S_1$ surface. Figure 1 illustrates the cross sections in both the $xy$ plane and the $xz$ plane of a few $R$ surfaces for the case $\mu=0.4$ and $\omega=0$, 2, 4 and 8. The case $\omega=0$ is simply the $S_1$ surface for $\mu=0.4$. The elongated shape of the cross sections in the $xz$ plane is easy to understand because those particles near the equatorial plane that have the highest linear velocities due to non-synchronous rotation are the easiest to be ejected out of the $S_1$ surface.

However, it should be noted that the $R$ surfaces represent neither the limiting nor equilibrium surface. Particles below the $R$ surface for a

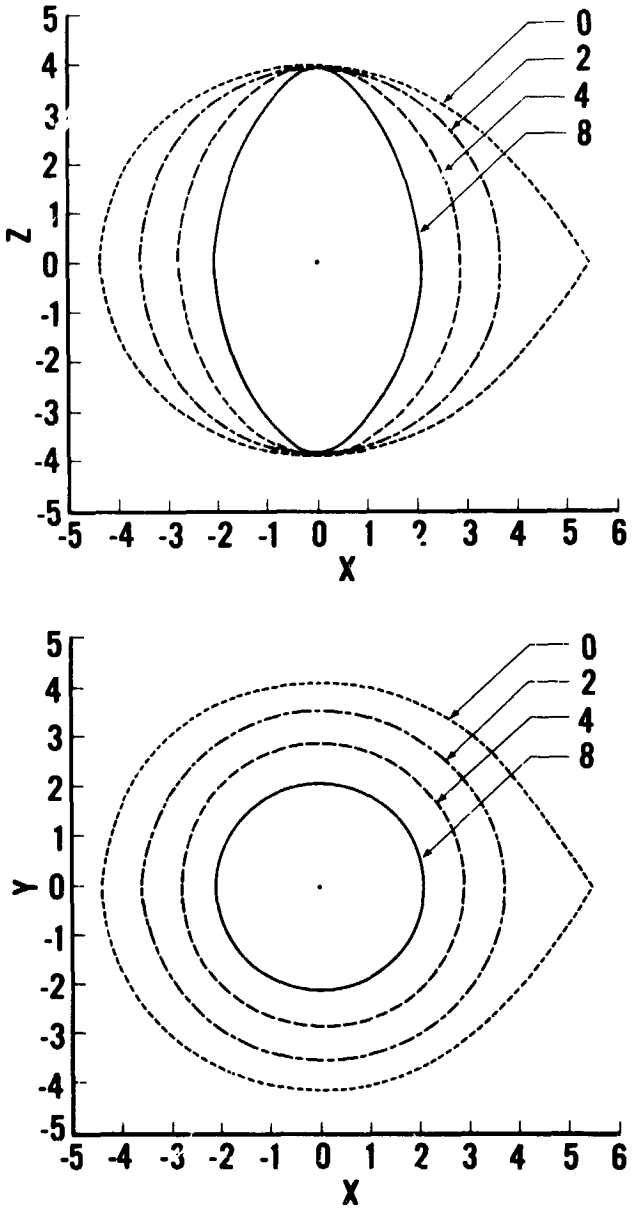


FIGURE. 1—The $R$ surfaces for different values of $\omega$ (0, 2, 4, 8) for $\mu = 0.4$. The $R$ surfaces are defined by equation (14). The case $\omega = o$ represents simply the innermost contact surface (denoted by $S_1$). When the rotation of a component star is not synchronous with its orbital motion, the gaseous particles above the $R$ surface may escape the $S_1$ surface and are replaced by gaseous particles moving out from below the $R$ surface. This process will go on until the star finally becomes synchronized to its orbital motion.

given value of $\omega$ can move up although they cannot escape through the $S_1$ surface without collisions. Statistically, we can state that most particles that are originally located above the $R$ surface are lost and are replaced by particles coming from below the $R$ surface. These new particles will naturally fill up the entire lobe of the $S_1$ surface. Therefore, the limiting surface of the $1-\mu$ component is still given by the $S_1$ surface. Since the angular momentum per unit mass due to the axial rotation of the $1-\mu$ component decreases downward in the star if it rotates as a rigid body, the new material above the $R$ surface will rotate less rapidly (with respect to the $xyz$ system) than the old material before the letter's escape. The simultaneous transfer of mass from below the $R$ surface to above the $R$ surface and from inside the $S_1$ surface to outside the $S_1$ surface will continue until the orbital revolution and the axial rotation become synchronize. Perhaps this axial rotation become synchronized. Perhaps this is one of the most effective mechanisms for synchronizing orbital revolution and axial rotation of close binary stars. Therefore, non-synchronization observed in those close binaries must be a temporary phenomenon triggered by rapid evolution of the component star itself as is suggested by Kopal (1959). But even at the time the two kinds of motion are temporarily out of step, the shape of the component is still given by the $S_1$ surface according to the present analysis.

Finally, one may question our argument on the ground that it has not proven that the particles are necessarily flying away from the star. If all particles on some surface of a non-synchronously rotating star should tend to move inward, this surface could be regarded as a stable surface for the star. This is however not true because when the particles move inward they collide with other particles. Since the average $C$ value (the $C$ value of each particle being defined by Eq. [12]) of all particles participating in a collision remains constant (Huang 1965) and since directions of the velocities will be modified after the collision, the chance of escape from the surface increases with time whatever are the directions of their initial velocities (in the $xyz$ system). Therefore, our conclusion about the non-synchronously rotating star is valid without qualification for the Roche model.

It is my pleasure to note my thanks to Mr. Clarence Wade, Jr. who has performed the computation involved in obtaining diagrams in Figure 1.

## REFERENCES

HUANG, S. -S., 1965, Ap. J., **141**,

KOPAL, Z., 1956, Ann. d'Ap., **19**, 298.

KOPAL, Z., 1959, "Close Binary Systems" (London: Chapman and Hall).

KRUSZEWSKI, A., 1963, Acta Astronomica, **13**, 106.

KUIPER, G. P., 1941, Ap. J., **93**, 133.

LIMBER, D. N., 1963, Ap. J., **138**, 1112.

MOULTON, F. R., 1914, "An Introduction to Celestial Mechanics" 2nd ed. (New York: Macmillan) chap. 8.

PLAUT, L., 1959, Pub. A.S.P. **71**, 167.

PLAVEC, M., 1958, Liège Symposium No. 8 on Emission-line Stars, p. 411.

STRUVE, O., 1941, Ap. J., **93**, 104.

STRUVE, O., 1950, "Stellar Evolution" (Princeton: Princeton University Press).

STRUVE, O., 1958, Pub. A.S.P., **70**, 5.

STRUVE, O. and HUANG, S. -S., 1957, Occasional Notes R.A.S., **3**, 161.

SWINGS, P., 1936, Zs. f. Ap., **12**, 40.

# AN INTERPRETATION OF ϵ AURIGAE*

SU-SHU HUANG†

A model of ϵ Aurigae has been proposed in order to explain the contradictory behavior of this star found in photometric and spectroscopic observations. This model which consists of a rotating gaseous disk that appears opaque when viewed edge-on resembles the one we have suggested for β Lyrae (Huang 1963). The success of this simple model to explain these two peculair stars which have defied other interpretations for so long, together with the fact that rotating gaseous rings are frequently associated with the primary component of the Algol-type binary systems (Joy 1942, also Sahade 1960) leads us to a belief that rotating gaseous rings or disks are the result of natural development of gases that are injected into the binary system by its component stars. This belief is further strengthened by our knowledge that such a rotating ring or disk is dynamically or hydro-dynamically feasible (Prendergast 1960, Huang 1964).

## I. INTRODUCTION

The binary ϵ Aurigae whose period is 27.1 years—one of the longest among eclipsing systems—gives every indication in its light curve of undergoing periodically total eclipses. But the spectrum of the eclipsed component, a F2 supergiant, can be observed persistently during the totality. These two seemingly irreconcilable phenomena have puzzled astronomers since the turn of the century. A serious attempt to resolve this incompatibility in the observational results may perhaps be traced to a paper by Kuiper, Struve and Strömgren (1937). They proposed an idea of making the huge eclipsing body—referred to as the I component—so tenuous as to be optically transparent to optical light. However, they argued that the ultraviolet radiation of the F-type supergiant would ionize the crescent-like thin layer of the I component that faces the F-type primary. The scattering by free electrons produced by ionization in this layer would then cut down the light from the F-type primary when the I component is in front, producing the phenomenom of eclipse. Since electron-scattering is frequency independent, the opacity in the crescent-like layer reduces the overall flux of the F component but does not change the spectral nature of the light. In this way, they are able to explain the difficulty we have mentioned before.

While this model has indeed resolved the long-standing difficulty, it introduces several new ones of equal, if not more, serious nature. Some of them have been mentioned in a recent work by Struve and Zebergs (1962).

Although the model by Kuiper *et al.* has been criticized, the idea of electron scattering as the cause of eclipse has persisted in the latter models by Struve (1956) and more recently by Hack (1961). This same idea has also strongly influenced the directions in which spectroscopic investigations of the star has been made (Kraft 1954).

Both Struve and Hack models may be regarded as modified versions of the original one by Kuiper *et al.* Struve introduced the idea that both components are surrounded by nebulous gases that fill the respective lobe of the inner contract surface of the system. These nebulous gases are supposed to cause gas streaming from one component to another and vice versa. Struve attributed the apparent splitting of lines observed before and after total eclipse to the presence of these gaseous streams. Except for this, Struve's interpretation of this peculiar system follows the same line of thought as in their previous paper. Consequently, the basic difficulties of eclipse by electron scattering are not removed.

*Published in *The Astrophysical Journal* 141:976, April 1965.

†Goddard Space Flight Center and Catholic University, Washington, D. C.

Hack's model does introduce a new concept. She proposed a hot secondary star of an effective temperature reaching 20,000°K. According to her, it is this hot star that is responsible for the ionization of gases in the shell or ring around it. The phenomenon of eclipse is then attributed to the intervention of this shell or ring between the primary F2 component and the observer.

It is more convincing to have an O or a B star around to do the work of ionization than an F2 star. But the introduction of a hot secondary meets other difficulties as we shall see in the following ways.

The depth of the eclipse during the apparent totality is about 0.8 magnitudes, which corresponds to an optical thickness of 0.74 over the entire spectral frequencies, if we assume that the eclipse is due to obscuration of the entire F component by the shell or ring. It requires $10^{24}$ of electrons in the column of unit cross-section and of a length equal to the thickness of the shell or ring. Since hydrogen is the dominant constituent, there will be approximately $10^{24}$ atoms in each column. Now, how could one explain that these atoms in their ionized states do not impress some additional spectroscopic feature on the light that passes through them? With ionizing radiation coming from a star of 20,000°K one would expect to observe spectral lines arising from such atoms as neutral or ionized helium, ionized oxygen, nitrogen, etc. that correspond to those found in the early-type supergiant stars. None have been observed. What have been actually observed, such as doubling and strengthening of lines in certain phases during eclipse, only show that the excitation level of the absorbing medium associated with the eclipsing body is not greatly different from that of the primary F2 atmosphere. Indeed, it has been specifically pointed out in the paper by Kuiper *et al.* that the lines associated with the secondary component and observed during eclipse are approximately, though not identically, the same as the normal lines of the F2 star.

Although it may be argued that compared with the F2 supergiant component, the hot star proposed by Hack is too faint to be seen in the visible region even during eclipse, it is difficult to comprehend why it has not been detected in the ultraviolet region. All these questions impair the otherwise attractive proposal by Hack.

From what has been said before, we cannot help but conclude that in spite of various modifications and refinements made since its inception. the electron scattering theory of the eclipse of $\epsilon$ Aurigae cannot explain this binary system in an internally consistent way.

Other theories of eclipse have been suggested in the meantime, but according to Hack (1961), none of them can explain the spectroscopic behavior of the system. However, it should be noted that Kopal's (1955) theory of attributing the opacity to solid particles did introduce a new conception of a ring structure which has been followed by Hack herself.

## II. A PROPOSED MODEL

The success of our interpretations of $\beta$ Lyrae by the introduction of an opaque gaseous disk rotating around its secondary component (Huang 1963) has led us to examine whether the same kind of model may be used for $\epsilon$ Aurigae, because in many respects the two peculiar binary systems show a similar behavior. Their similarities are: (1) The light from the primary component can be seen during the entire duration of eclipse while the spectrum of the secondary component itself has never been observed at any phase. (2) Additional lines appear during eclipse. These lines are, in both system, displaced towards the red end before the principal mid-eclipse and towards the violet end after mid-eclipse. (3) Light shows fluctuations, especially during eclipse, and (4) both show emission features.

However, there are also differences between these two systems. In the first place, the magnitudes of wavelength shifts of those additional lines observed during eclipse are different. In the case of $\beta$ Lyrae, the radial velocities corresponding to the shifts are of the order of 100–300 km/sec, while in the case of $\epsilon$ Aurigae the velocities are perhaps of the order of 30–50 km/sec. This difference actually confirms our conviction that the two systems are similar, if we remember that the period of $\beta$ Lyrae is only about 13 days while that of $\epsilon$ Aurigae is about 27.1 years. Thus, for the purpose of a similarity consideration, we must compare the stream velocities in terms of the respective orbital velocities of the component stars. Then the stream velocities in the two systems are of the same order of magnitude.

Another difference between these two systems comes from the fact that $\beta$ Lyrae shows a secondary eclipse but $\epsilon$ Aurigae does not. This difference can be readily explained on the basis of our model of an opaque disk, as we shall see presently.

Figure 1 shows the model we propose for $\epsilon$ Aurigae. The obscuration of the primary component by the rotating gaseous disk causes an eclipse which would look, in the light curve, like

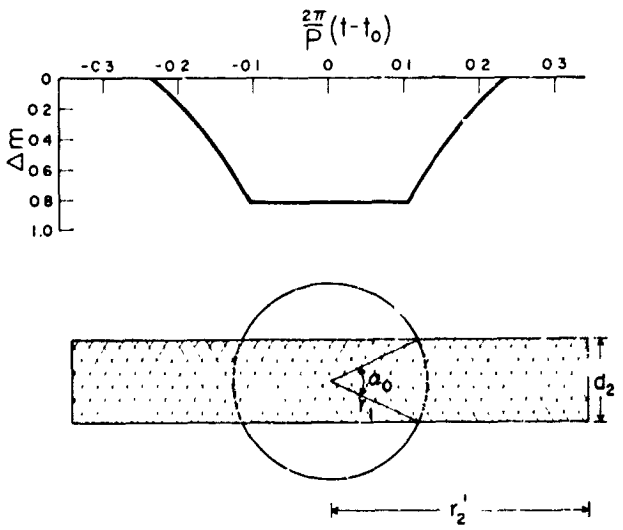


FIGURE 1.—A schematic diagram of our model for $\epsilon$ Aurigae and its resulting light curve during eclipse. It is assumed that we observe this sytem edge-on. Consequently, the rotating gaseous disk around the secondary component will appear like a dark rectangle which obscures the primary component during eclipse. The light curve at the top of the figure is derived by assuming a uniform stellar disk.

total but the light from the primary will continuously be seen even at the apparent totality. We suggest that the inclination, $i$, of this system is very near to 90°. Thus, we see only the edge of the disk; the secondary component itself cannot be seen because it is hidden in the disk. Because of this inclination neither do we receive any radiation from the primary reflected by the disk. As a result there will be no secondary eclipse. On the other hand, we have suggested in the previous paper that $\beta$ Lyrae has an inclination which differs appreciably from 90° so that we can see the secondary star itself as well as the light reflected by the rotating gaseous disk. Consequently, we are able to observe a secondary eclipse.

Because of the difference in inclination, the shape of minimum differs in these two systems too. In the case of $\beta$ Lyrae, the projected area of the disk will be an elongated ellipse, resulting in a curved minimum in the light variation. In the case of $\epsilon$ Aurigae, the projected area would be a rectangle (as shown in Figure 1), producing a flat minimum.

The sizes of the primary component and the opaque disk may be determined from the light curve. Let us, for the sake of illustration, assume that the stellar disk of the primary component is uniform in brightness and the edge of the disk we actually face is completely dark. We can now determine the radii, denoted respectively by $r_1$ and $r_2'$ of both the primary component and the disk around the secondary component as well as the thickness of $d_2'$ of the disk. All these quantities will be measured in terms of the mean separation between the two components of the system.

Different investigators gave different values for the duration of eclipse, $D$, and the of totality, $d$. We shall follow Plaut's (1950) values $D=0.0760$ and $d=0.340$, which yield after a simple calculation,

$$r_1=0.065 \text{ and } r_2'=0.171. \tag{1}$$

In order to determine $d_2'$ we must use the observed depth of eclipse during the apparent totality. If we denote by $\alpha_0$ the angle subtended at the center of the primary by the two points of intersection, all projected on the celestial sphere, between the boundary lines of the opaque disk and the primary component during eclipse (see Figure 1), the maximum light $L_1$ and the minimum light $L_2$ of the system are related by

$$\frac{L_2}{L_1}=\frac{\pi-\alpha_0-\sin\alpha_0}{\pi} \tag{2}$$

where

$$\sin\left(\frac{\alpha_0}{2}\right)=\frac{1}{2}\frac{d_2'}{r_1} \tag{3}$$

Since the observed depth of minimum is 0.81 mag., equation (2) gives $\alpha_0=0.881$ which in turns yields

$$d_2'=.055 \tag{4}$$

## III. INTERPRETATION OF THE LIGHT CURVE

As an illustration that the present model can predict a light curve very much like the one actually observed, we shall consider a central eclipse ($i=90°$) of a uniformly bright stellar disk of the primary component by the dark projection of the rotating disk, shown schematically in Figure 1. If we denote by $\delta$ the apparent distance between the center of the primary and the center of the opaque disk and if we let

$$\delta_1=r_1+r_2', \qquad \delta_2=r_1\cos\tfrac{1}{2}\alpha_o+r_2', \qquad (5)$$
$$\delta_3=r_2'-r_1\cos\tfrac{1}{2}\alpha_o, \qquad \delta_4=r_2'=r_1,$$

where $r_1$, $r_2'$ and $\alpha_o$ have been determined in the previous section, the light curve predicted on this model is given by

$$\frac{L_2}{L_1}=1-\frac{1}{2\pi}(\alpha_1-\sin\alpha_1), \quad \delta_2\leq|\delta|\leq\delta_1 \qquad (6)$$

$$\frac{L_2}{L_1}=1-\frac{1}{2\pi}(\alpha_o-\sin\alpha_o)-\frac{d_2'}{\pi r_1^2}(\delta_2-\delta),$$
$$\delta_3\leq|\delta|\leq\delta_2 \qquad (7)$$

and

$$\frac{L_2}{L_1}=1-\frac{1}{\pi}(\alpha_o+\sin\alpha_o)+\frac{1}{2\pi}(\alpha_2-\sin\alpha_2),$$
$$\delta_4\leq|\delta|\leq\delta_3 \qquad (8)$$

where

$$\cos\frac{1}{2}\alpha_1=1-\frac{\delta_1-\delta}{r_1} \text{ and } \cos\frac{1}{2}\alpha_2=1-\frac{\delta-\delta_4}{r_1}$$

For $o\leqslant|\delta|\leq\delta 4$, $L_2/L_1$ has already been given in equation (2).

The light curve according to these equations has been computed with the numerical values given by equations (1) and (4) and is plotted at the top of Figure 1. There is a general agreement between this predicted curve and the actually observed one (Güssow 1936).

It may be noted parenthetically that this interpretation of the light curve of $\epsilon$ Aurigae requires only that the rotating disk is opaque when viewed along the edge. Whether it is transparent or opaque in its vertical direction, does not matter in our interpretation. Indeed, we have no observational means to ascertain the optical depth in its vertical direction.

As has been pointed out by Fredrick (1960), the light curve shows a slight asymmetry. On the basis of our model, the asymmetry in the light curve reflects either a corresponding asymmetry in the thickness of the rotating disk or an additional absorption by gaseous stream above and below the rotating disk. Physically, it is difficult to envisage a permanent asymmetry in the thickness of the disk. Therefore it is most probable that the asymmetry is caused by the gaseous stream. If we assume that there is a gaseous stream flowing out from the primary component through the Lagrangian point into the secondary lobe of the innermost contact surface (Kuiper 1941), the gaseous stream will circulate around the secondary component above and below the main body of the rotating disk. As the gaseous streams circulate around the secondary component in the same sense as the rotation of the disk, which is in turn supposed to be rotating in the same sense as the binary motion, we would expect that they will gradually coalesce into the disk itself as a result of collisions. It is then not difficult to see that at any moment more gas would be found in the rear side than in the front side of the secondary component, giving rise to an asymmetry in absorption in agreement with the observed result. In this respect the behavior of the gaseous streams outside the main body of the rotating disk resembles closely what has been suggested for $\beta$ Lyrae, which shows an asymmetric primary eclipse, with the decline steeper than the rise. We have attributed this asymmetry also to obscuration of gases just streaming out from the primary component, this obscuration making the eclipse last longer, and consequently show slower decline than would be the case of intervention of a simple disk. According to this interpretation, the light curves of both $\epsilon$ Aurigae and $\beta$ Lyrae before mid-eclipse are perhaps less distorted by gaseous streams outside the rotating disk than those after mid-eclipse.

Other interesting facts found in this system are, according to Güssow (1936) and Fredrick (1960), that the light fluctuation far away from eclipse does not exceed 0.1 mag., that in 3–5 years before and after eclipse the variation may get as large as, but seldom 0.2 mag. and that in totality, the fluctuation may reach 0.3 mag. or even slightly larger. Such a manner of variations

in light follows also quite naturally from our model. While the intrinsic variation of light far away from eclipse is expected from the supergiant F2 primary itself, the greater fluctuation in light near and during eclipse only indicates the unsteadiness of gaseous streams on both sides of the rotating disk.

## IV. INTERPRETATION OF SPECTROSCOPIC RESULTS

That $\epsilon$ Aurigae shows an $H_\alpha$ emission has long been known (Adams and Sanford 1930). More recently, Wright and Kushwaha (1958) have made an extensive study of the structure of this $H_\alpha$ line both inside and outside the last eclipse. According to them, the two emission wings are almost equal in intensity outside eclipse. Moreover, the central absorption gives the same radial velocity as the absorption lines of *Fe*II, *Ba*II, and *Y*II in all phases outside eclipse. This result suggests that the material that produces the emission feature moves with the primary.

Moreover, Wright and Kushwaha have found that just before and during ingress the emission wing towards violet is usually stronger than that towards red and during egress, the reverse is true. At the time of totality, the absorption becomes dominant.

The $H_\alpha$ emission is produced by gases moving with the primary component, but we still do not know how they are distributed in space around the primary component. The line profile outside eclipse appears to suggest a rotating gaseous ring like the one observed in many an Algol-type binary system (Joy 1942; also Sahade 1960). However, the behavior of this emission line found in $\epsilon$ Aurigae during eclipse differs from what has been observed in the Algol-type variables. In the latter, the emission wing toward violet decreases in strength when the system enters into eclipse, but in $\epsilon$ Aurigae, the same wing increases in strength. Similarly, in egress, the two cases show variation in the relative intensity of the two emission wings in opposite directions. Two hypotheses as regards the distribution of emitting gases may be proposed to explain the behavior of $H_\alpha$ emission found in $\epsilon$ Aurigae in and out of eclipse. (1) The emission indeed comes from a gaseous ring rotating around the primary but the sense of rotation is opposite to the orbital revolution of components in the system. (2) Emission is produced by expanding gases ejected from the primary component. It is interesting to note that Adams and Sanford (1930) did find that $H_\alpha$ showed then as an emission line with an absorption border on its violet edge, indicating outward motion of gases. Consequently, Beals (See Hack 1961) classified it as a $\rho$ Cygui star.

According to Wright and Kushwaha the weak emission feature that occurs during totality seems to correspond to the velocity of the system and could be due to the tenuous gases enveloping the entire binary.

White the $H_\alpha$ emission mainly comes from gases associated in whatever way with the primary component, the complicated absorption feature of this line observed during eclipse is due to gases spilled above and below the main body of the disk around the secondary component.

It is reasonable to assume that the distribution of gases around the secondary component is not confined to the disk itself. However, for the same reason that the material density in the galactic plane falls off rapidly in the polar directions, the density around the secondary component must also decrease rapidly with the perpendicular distance. At places not too far away from the main body of the disk, the gaseous distribution would be so rare that it is no longer opaque to the continuous radiation but it may still produce line absorption. Therefore, we should expect to observe it through spectroscopic study. Indeed, according to our model, it is this gas distribution that produces the additional absorption that modifies the profile of $H_\alpha$ continuously with phase during eclipse. Thus, during ingress, additional absorption which occurs in the red side of the normal position makes the emission wing toward violet appear stronger than the other. A similar argument leads to the reverse conclusion at the time of egress. During totality the light from the primary passes through a large amount of gases, resulting in a dominantly absorption line as observed. In this way Wright and Kishwaha's results can be satisfactorily explained on the present model.

Because of the appearance of $H_\alpha$ emission in its spectrum, it has been proposed (Wright and Kishwaha 1958) that the excitation might be due

to a hot secondary, since under normal conditions, no emission at $H_\alpha$ appears in the spectra of a star as late as spectral type F of the primary component. As we have seen before, Hack has incorporated this suggestion in her theory in order to explain the ionization of gases in the shell or ring around the secondary. In section I, we have seen that a hot secondary introduces some new difficulties. Now we have found that the $H_\alpha$ emission comes from gaseous distribution associated with the primary instead of the secondary. Hence, the hypothesis of a hot secondary made in order to explain $H_\alpha$ emission becomes even less satisfactory than the case if the emission were associated with the secondary.

If the gases spilled over the disk give rise to absorption that cuts into $H_\alpha$ emission, we would expect during eclipse the appearance of lines belonging to other elements than hydrogen. Indeed, the indication of such an additional absorption long been known. According to Kuiper *et al*, the spectral lines of many elements become asymmetric during ingress by the presence of a strong core on the red side. The degree of asymmetry increases, reaches a maximum at second contact and then diminishes until mid-eclipse when each line becomes symmetric as it is outside eclipse. However, the intensities of lines at mid-eclipse are somewhat stronger than those outside eclipse. After mid-eclipse, the lines become asymmetrical again, but with a strong core on the violet side this time. This asymmetry increases rapidly until it reaches third contact. The asymmetry is obviously due to the presence of a double structure (Adams and Sanford 1930) and indicates the additional line absorption by gases spilled over from the disk. The sense of the Doppler shift of these lines agrees again with what one would expect from gaseous streams rotating in the same sense as the orbital revolution.

In the previous section we have attributed the asymmetry of the light curve also to gaseous streams which are located perhaps closer to the disk than those giving rise to absorption lines. We have suggested that the gaseous streams must be more complicated and extend a larger region in the rear side than in the front side of the secondary. Accordingly, we would expect the structure of absorption lines observed after mid-eclipse to be more complicated than that observed before mid-eclipse. Struve and Pillans' (1957) observational results appear to bear this prediction out. They have found that at the very end of totality, the absorption lines show a remarkable amount of structure not previously observed in the star. Some lines are triple, while others show a double structure, indicating gaseous streams, just coming out from the primary before collision which would have erased the velocity differences of the streams.

## V. THE F2 SUPERGIANT ATMOSPHERE, ITS MASS EJECTION AND TURBULENT VELOCITIES

Finally, we may say a few words about the atmosphere of the F2 supergiant primary. Whatever is the mass ratio of the system, it is reasonably certain that the size of the primary component derived in Section II must be small compared with the innermost contact surface (e.g. Kuiper 1941), which will be referred to hereafter as the $S_1$ surface. Indeed, the light curve outside eclipse does not indicate any distortion due to ellipticity. On the other hand, both spectroscopic and photometric results indicate that mass is continuously flowing out of the primary lobe of the $S_1$ surface into the secondary lobe. It follows that at the photospheric surface, the star must steadily eject matter to keep the flow of gas from the primary lobe to the secondary lobe of the $S_1$ surface. Since the photosphere is well below the $S_1$ surface, the effect of its comparison must be small. Consequently, mass ejection at the stellar surface (i.e. photosphere) must be intrinsic to this F2 supergiant primary and should not be attributed to the interaction within a binary.

Thus, between the photosphere and the corresponding lobe of the $S_1$ surface, the vast volume must be filled with a tenous atmosphere. Its extension must be several times the stellar radius; through the extended atmosphere the primary is losing its mass. The picture thus derived agrees completely with what Deutsch (1956, 1960) has found in many red giant and supergiant stars and confirms the general belief that a supergiant—whatever is its spectral type—is always ejecting mass.

Violent motions have always been found in atmosphesre of supergiant stars (e.g. Huang and Struve 1960). This is especially true in the primary of $\epsilon$ Aurigae (Wright and van Dien 1949;

Hack 1959). However, the nature of the observed motion has never been clearly understood, although frequently but rather vaguely we have attributed it to some kind of prominence activities. With the conception of mass ejection by the supergiant star reasonably established, we can now understand why violent motion should always be associated with its atmosphere. Indeed, the mass ejection from the stellar surface, presumably due to convective currents below, acts as a stirring mechanism of the atmosphere over the photosphere. The ejection creates a velocity field in the atmosphere which also makes the latter very extended.

## REFERENCES


ADAMS, W. S., and SANFORD, R. F., 1930, Pub. A.S.P., **42**, 203.

DEUTSCH, A. J., 1956, Ap. J., **123**, 210. 1960, "Stellar Atmospheres," ed. J. L. Greenstein, (Chicago: University of Chicago Press), Chap. **15.**

GÜSSOW, M., 1936, Veröff Berlin-Babelsberg, **11**, No. 3.

HACK, M., 1959, Ap. J., **129**, 291. 1961, Mem. Soc. Astr. italiana, **32**, No. 4.

HUANG, S. -S., 1963, Ap. J., **138**, 342. 1964, to be published.

HUANG, S. -S., and STRUVE, O., 1960, "Stellar Atmospheres' ed. by J. L. Greenstein (Chicago: University of Chicago Press), Chap. **8.**

JOY, A. H., 1942, Pub. A.S.P., **54**, 35.

KOPAL, Z., 1955, Comm. Coll. Intern. d'Astrop. Liége **6**, 241.

KRAFT, R. P., 1954, Ap. J., **120**, 391.

KUIPER, G. P., 1941, Ap. J., **93**, 133.

KUIPER, G. P., STRUVE, O. and STRÖMGREN, B., 1937, Ap. J., **86**, 570.

PLAUT, L., 1950, Pub. Kapteyn Astr. Lab. Groningen No. 54.

PRENDERGAST, K. H., 1960, Ap. J., **312**, 162.

SAHADE, J., 1960, "Stellar Atmospheres," ed. J. L. Greenstein (Chicago: University of Chicago Press), Chap. **12.**

STRUVE, O., 1956, Pub. A.S.P., **68**, 27.

STRUVE, O. and PILLANS, H., 1957, Pub. A.S.P., **69**, 169.

STRUVE, O. and ZEBERGS, V., 1962, "Astronomy of the 20th Century," (New York: Macmillan Co.)

WRIGHT, K. O. and DIEN, E. VAN, 1949, J.R A.S. Canada **43**, 15.

WRIGHT, K. O. and KUSHWAHA, R. S., 1958, Comm. Coll. Intern. d'Astrop. Liége **8**, 421.

# THE MOTION OF GASEOUS STREAMS IN THE BINARY SYSTEM*

SU-SHU HUANG†

We have studied several problems in connection with the gaseous flow in the close binary system. First, the statistical property of the Jacobian constants of colliding particles in the system is examined and a conversation law for their mean value established. Then the velocity-independent nature of the rate of change in angular momentum of a particle moving in the binary system is pointed out. These properties prompt us to derive for the gaseous flow a set of differential equations that provide a point of view lying in the middle between the orbital approach (which neglects both pressure and collision) and the hydrodynamic approach (which includes both) because our equations take into account the collision but not the pressure. The equations have been solved under the same approximation as Prendergast (1960) has assumed and have been found to yield a similar result as was obtained by him from the hydrodynamic equations.

Because of our emphasis on the Jacobian constant and angular momentum in the treatment of gaseous flow we have called attention to the fact that some combinations of these two physical quantities are incompatible in a certain region of space which we have called the forbidden zone.

Finally, the formation, the evolution and the significance of rotating rings observed in many Algol-type eclipsing binaries are discussed in an effort to understand the mode of ejection of matter from the secondary surface.

## I. INTRODUCTION

The problem of gaseous streams observed in some binary systems has been studied theoretically either as individual bodies moving in orbits independently of each other (Kopal 1959, Gould 1959) or as an aerodynamical flow (Prendergast 1960). Both approaches encounter difficulties, though of entirely different nature. In the present paper, we shall call the attention to a few general properties of the motion of gaseous particles in the binary systems, which lead us to a theory that somewhat reconciles these two fundamentally different approaches and thereby makes the flow problem easier to comprehend.

## II. STATISTICAL PROPERTY OF THE JACOBIAN CONSTANTS DURING A COLLISION OF PARTICLES

One of the differences between the two approaches mentioned in Section I concerns the collision of particles. While the neglect of this important process makes the orbital approach unrealistic, some results obtained in celestial mechanics of the motion of an infinitesimal body in a gravitational field of two revolving components has its physical significance. This is because of the statistical property of the Jacobian constants that we will discuss in this Section.

Let us assume that the two stars are revolving around each other in circular orbits. This is generally true for close binaries (Struve 1950). Thus, a motion of a particle in such a system is identical to what is treated in the restricted three-body problem in celestial mechanics (e.g., Moulton 1914; Brouwer and Clemence 1961). Following the standard treatment of the problem we shall choose as the unit of length, the separation between the two components, as the unit of mass, the total mass of the two components, and as the unit of time, the perior of the orbital motion of the two components divided by $2\pi$. In such a unit system the gravitational constant is one. Let us now denote by $\mu$ the mass of the secondary component. Thus, the mass of the primary will be $1-\mu$. If, furthermore, a rotating coordinate system $xyz$ is

*Published in *The Astrophysical Journal*, 141(1):201–209, January 1, 1965.

†Goddard Space Flight Center and Catholic University, Washington, D. C.

so chosen that its origin is at the center of mass of the two components, its $x$-axis coincides at all times with the line joining the two components and its $z$-axis is perpendicular to the orbital plane of the stars, then the coordinates of the primary will be $x_1=-\mu, y_1=o, z_1=o$ and those of the secondary will be $x_2=1-\mu, y_2=o, z_2=o$ in consistency with the adopted unit system.

The equations of motion of the third infinitesimal body in the restricted three-body problem admits an integral, frequently known as the Jacobian integral, as follows:

$$C=2U-(\dot{x}^2+\dot{y}^2+\dot{z}^2) \tag{1}$$

where

$$U=\frac{1}{2}(x^2+y^2)+\frac{1-\mu}{r_1}+\frac{\mu}{r_2} \tag{2}$$

Here $r_1$ and $r_2$ are respectively the distances of the infinitesimal body from the primary $(1-\mu)$ and the secondary $(\mu)$ component, while $(x,y,z)$ the three vector components of $\vec{r}$, are the coordinates of the infinitesimal body. The dot represents as usual the time derivative. The integration constant $C$, is known as the Jacobian constant.

We can transform equation (1) into a stationary system. Let us now consider a collision of $n$ particles of mass, $m_i(i=1, 2 \ldots n)$. Since we have particles of atomic sizes, the coordinates may be regarded as the same for all colliding particles at the instant of collision. Moreover, the total kinetic energy of the colliding particles conserves during an elastic collision. It follows from these considerations as well as the definition of $C$ by equation (1) that

$$\sum_{i=1}^{n} m_i C_i' = \sum_{i=1}^{n} m_i C_i \tag{3}$$

where $C_i$ and $C_i'$ are respectively the Jacobian constant of the $i$-$th$ particle before and after the collision. Thus, if we define an average $C$, such that

$$<C>\sum_{i=1}^{n} m_i = \sum_{i=1}^{n} m_i C_i, \tag{4}$$

$<C>$ will be an invariant under the physical processes of elastic collisions. However, it may be noted that the dispersion of $C$'s from their average value will in general change after each collision.

For inelastic collisions an equation connecting various $C_i$ and $C_i'$ can always be obtained from the energy consideration if we know the detailed process of the collision. We shall assume in the present paper that the collisions that take place among particles in the binary system are statistically elastic, i.e., endoergic collisions balancing exoergic ones.

As a result of the constancy of $<C>$ during collision, the problem of gaseous flow is considerably simplified because we have now a macroscopic quantity, $<C>$, to deal with instead of following the courses of numerous particles in the system. Thus, the gaseous particles must maintain a constant value of $<C>$ in their stream motion. Indeed, Prendergast (1960) has shown that $C$ is a constant along a stream line. This situation resembles the introduction of the concept of temperature and pressure which simplifies our study of the chaotic motion of molecules in gases in free space. Therefore, whatever is the nature of ejection that occurs on the stellar surface, the mean value of $C$'s of ejected particles and their dispersion serve as two of the most characteristic indices of the mode of ejection as regards the course of their subsequent motion.

It should be noted, however, that although the gaseous particles maintain a constant $<C>$, the mean flow does not follow the orbit derived from the equations of motion of the three-body problem. It is physically obvious that all those loops, cusps, sudden reversal in the direction of motion, and other erratic behavior found in the orbits of the three-body problems must be completely erased by collisions.

## III. THE RATE OF CHANGE OF ANGULAR MOMENTUM

The angular momentum (the $z$-component) per unit mass of the third body with respect to the center of mass of the binary system will be denoted by $h$. It is given by:

$$h=x^2+y^2+x\frac{dy}{dt}-y\frac{dx}{dt} \tag{5}$$

and varies with time because the third body is continuously interacting with the two revolving component stars.

Although $h$ varies with time, there are two points which make it physically significant. First, the total angular momentum is conserved among the colliding particles if the collision takes place rapidly. Secondly, it can be easily shown from the equations of motions in the restricted three-body problem that

$$\frac{dh}{dt}=\mu(1-\mu)y\left(\frac{1}{r_1^3}-\frac{1}{r_2^3}\right). \tag{6}$$

The significance of equation (6) derives from the fact that $^{dh}/_{dt}$ is a function of coordinates of the third body only, being independent of its velocity. Moreover, it is anti-symmetric with respect to the $x$-axis and to the line bisecting the separation segment between the two finer bodies. Thus, it vanishes on these two lines. Here we see physically why five Lagrangian points all lie on either of these two lines. It follows that any steady flow in a closed curve must cross either one or both of these lines so that $h$ will recover to its original value after the completion of the circuitous flow. Indeed, this is the case of rotating gaseous rings frequently observed around the primary component in many an Algol-typebinary system (Joy 1942, 1947; also Sahade 1960).

In the three dimensional case, $^{dh}/_{dt}$ vanishes in the $XZ$ plane and in the plane bisecting the line joining the two components. Thus, if we divide space into four regions by these two planes the sign of $^{dh}/_{dt}$ is positive in the two regions and negative in the other two.

## IV. GASEOUS FLOW DERIVED FROM THE C AND h CONSIDERATIONS

In the two dimensional case, a knowledge of $C$ and $h$ at every point defines completely the flow pattern. Therefore, a velocity vector field of gaseous motion in a binary system can be defined by two scalar fields of $h$ and $C$. Since the average values of $C$ and $h$ do not change by collision, we may write

$$\frac{\partial C}{\partial t}+\vec{u}\cdot\nabla C=o \tag{7}$$

from the constancy of $C$ and

$$\frac{\partial h}{\partial t}+\vec{u}\cdot\nabla h=\mu(1-\mu)\left(\frac{1}{r_1^3}-\frac{1}{r_2^3}\right) \tag{8}$$

from equation (6) when we follow the stream lines. In writing these equations where $u$ denotes velocity at points $(x, y)$ we have made an additional assumption that $C$ and $h$ are continuous over the plane. In this way, we have derived two flow equations from the results of celestial mechanics.

By imposing the continuity condition of $C$ and $h$ over space we are able to take advantage of the result derived from celestial mechanics but at the same time to discard as meaningless the seemingly erratic and infinitely varied forms of orbits that one may actually obtain by a straight integration of the equations of motion in the three-body problem. Thus, equations (7) and (8) are proposed here purely from physical arguments of conservation laws in collisions. A mathematical derivation from hydrodynamic equations is given in the Appendix.

Since the pressure is not included in equations (7) and (8), the present formulation of the flow problem lies between the orbital approach (which neglects both pressure and collision) and the bona fide hydrodynamic equations of flow (which include both). Thus, the present treatment is mathematically equivalent to the hydrodynamic approach when the pressure is neglected. In presenting the problem in this manner we gain a better physical insight because both $C$ and $h$ are physical quantities.

Actually an inclusion of pressure would make the problem very difficult. Indeed, Prendergast (1960) who started directly from hydrodynamic equations also neglected the pressure term when he came to the stage of solving the equations. Thus, the equations (7) and (8) should be equivalent to what Prendergast has used, although the basic approach is different.

What we will show in the following is that we can obtain a similar solution as obtained previously by Prendergast. Also by following the present derivation we can see very clearly the conditions under which the solution will be valid.

Following Prendergast, we shall consider the two-dimensional case, neglect the velocity component at right angles to the zero-velocity curves and choose a right-handed orthogonal curvilinear coordinate system $(\xi, \eta, z)$ where $\xi$ is the label of the zero-velocity curves, namely

$$U=\xi, \tag{9}$$

$U$ is given by equation (2) and $\eta$ is an angular measure along the zero-velocity curve. If we now denote $Q_\xi$ and $Q_\eta$ the metric coefficients corresponding to this coordinate system, we can express equations (7) and (8) in this new system as follows:

$$\frac{u_\xi}{Q_\xi}\left[1-\left(u_\xi\frac{\partial u_\xi}{\partial \xi}+u_\eta\frac{\partial u_\eta}{\partial \xi}\right)\right] -\frac{u_\eta}{Q_\eta}\left(u_\xi\frac{\partial u_\xi}{\partial \eta}+u_\eta\frac{\partial u_\eta}{\partial \eta}\right)=o \quad (10)$$

and

$$\frac{u_\xi}{Q_\xi}\left(\frac{\partial r^2}{\partial \xi}+r_\xi\frac{\partial u_\eta}{\partial \xi}+\frac{\partial u_\xi}{\partial \xi}u_\eta-r_\eta\frac{\partial u_\xi}{\partial \xi}-\frac{\partial r_\eta}{\partial \xi}u_\xi\right) +\frac{u_\eta}{Q_\eta}\left(\frac{\partial r^2}{\partial \eta}+r_\xi\frac{\partial u_\eta}{\partial \eta}+\frac{\partial r_\xi}{\partial \eta}u_\eta-r_\eta\frac{\partial u_\xi}{\partial \eta}-\frac{\partial r_\eta}{\partial \eta}u_\xi\right) =\mu(1-\mu)y\left(\frac{1}{r_1^3}-\frac{1}{r_2^3}\right) \quad (11)$$

if we assume a steady state of flow. Here the subscripts $\xi$ and $\eta$ denote respectively the components of the vector in the $\xi$ and $\eta$ direction.

If we neglect $u_\xi$ we obtain

$$\frac{\partial u_\eta}{\partial \eta}=o \quad (12)$$

from equation (10) and

$$\frac{u_\eta}{Q_\eta}\frac{\partial r^2}{\partial \eta}+\frac{u_\eta}{Q_\eta}\left(r_\xi\frac{\partial u_\eta}{\partial \eta}+\frac{\partial r_\xi}{\partial \eta}u_\eta\right)=\mu(1-\mu)y\left(\frac{1}{r_1^3}-\frac{1}{r_2^3}\right) \quad (13)$$

from equation (11). Combining equations (12) and (13) we obtain a second degree algebraic equation for $u_\eta$

$$\frac{u_\eta}{Q_\eta}\frac{\partial r^2}{\partial \eta}+\frac{u_\eta^2}{Q_\eta}\frac{\partial r_\xi}{\partial \eta}=\mu(1-\mu)y\left(\frac{1}{r_1^3}-\frac{1}{r_2^3}\right) \quad (14)$$

By neglecting $u_\xi$ in one of the two hydrodynamic equations of flow a $u_\xi^2$ in the other, Prendergast has also obtained and second degree algebraic equation for $u_\eta$. While the coefficients in the equation here (which involves $\partial r^2/\partial \eta$ and $\partial r_\xi/\partial \eta$) are completely different from those in Pendergast's equation, (which involves $\partial Q\eta/\partial_\xi$), both results are valid under the same approximation. Now it appears from equation (10) that in order to neglect $u_\xi$, $\partial u_\eta/\partial \eta$ must be small. This is the condition for the validity of our solution.

Physically we have started by assuming that the flow follows the zero-velocity curves, but once we have found $u_\eta$, according to equation (14) we immediately see that $u_\xi$ does not vanish because $\partial u_\eta/\partial \eta$ does not. So the flow cannot exactly follow the zero-velocity curves. Whether we can find a converging field of velocities for this steady state by an iterating process, we do not know. Neither has Prendergast commented on this possibility.

However, near the two finite bodies, the variations of velocity with $\eta$ is small, so the flow pattern obtained here represents a good approximation. This explains why gaseous rings are frequently observed around the primary component of many an Algol-type eclipsing binary.

In order to complete the analogy of the present calculation with Prendergast's, we may write equation (10) by neglecting $u_\xi^2$ and higher order terms, as follows

$$u_\xi=\left(\frac{Q_\xi}{Q_\eta}\right)u_\eta^2\frac{\partial u_\eta}{\partial \eta}\left(1-u_\eta\frac{\partial u_\eta}{\partial \xi}\right)^{-1}$$

We can now examine the asymptotic behavior of $u_\eta$ for small values of $r_1$ (or similarly of $r_2$). In the immediate neighborhood of the $1-\mu$ component, we may take the position of this component as the origin and use the polar coordinate system $(r_1, \varphi)$ where $\varphi$ is the angle that the radius vector $\vec{r}_1$ makes with the $x$-axis, being counted, as usual, positive in the counter-clockwise direction from the positive $x$-axis. The zero-velocity curves in the immediate neighborhood can be approximated by circles. Thus, we have

$$\xi=U\to\frac{1-\mu}{r_1},\ Q_\eta=r_1 \quad (15)$$

and

$$\eta=-\varphi \quad (16)$$

since $(\xi,\eta,z)$ is a right-handed coordinate system.

It can be easily shown that equation (14) reduces to

$$u_\eta^2-2r_1u_\eta-\frac{1-\mu}{r_1}=o, \quad (17)$$

under the approximation given by equations (15) and (16). We take the negative sign before the square root in the solution of this quadratic equation, because as Prendergast has pointed out, the velocity should vanish if the force vanishes. Retaining the dominant terms, we find the solution for small $r_1$

$$u_\eta = r_1 - \left(\frac{1-\mu}{r_1}\right)^{\frac{1}{2}}. \tag{18}$$

This asymptotic expression represents the Keplerian velocity in the neighborhood of the $1-\mu$ component in the rotating coordinate system.

In order to study the asymptotic behavior at large distances from both the components, we use the polar coordinates $(r, \theta)$ and expand all quantities in terms of $1/r$, $\theta$ being now the angle between the radius vector $\vec{r}$ and the $x$-axis. It can be shown that the angle that the normal to the zero-velocity curve makes with the radius vector $\vec{r}$ decreases as $1/r^5$. Consequently, we may take the radius vector as the normal to the curve as a first approximation for zero-velocity curves at large distances. Similarly, we can show that the radius of curvature may be set equal to $r$ if we neglect terms of $1/r^5$ and higher orders. With these approximations we can easily derive from equation (14)

$$u_\eta = -r, \tag{19}$$

if we remember that in this asymptotic case

$$\eta = \theta. \tag{20}$$

According to equation (19) the gas remains at rest in the stationary frame of reference. Thus, the asymptotic behavior in both cases is, as it should be, identical to what Prendergast has obtained.

The numerical evaluation of $u_\eta$ is not simple but it can be done. We shall illustrate it by computing values of $u_\eta$ at those two points in the flow around the $1-\mu$ component where a stream line intersects with the $x$-axis. At these two points we can take advantage of the simplification arising from the symmetry of the zero-velocity curves with respect to the $x$-axis.

Let point $A(x_o, o)$ be the one of these points on the right side of the $1-\mu$ component and point $B(x_o, o)$ the one on the other side. Thus, $x_o > -\mu$ at A and $x_o < -\mu$ at B. The relation between $x_o$, $r_1$ and $r_2$ at both A and B can be easily obtained.

Since $Q_\eta$ denotes the radius of curvature of the zero-velocity curve at A or B then we have in the immediate neighborhood of A or B

$$r^2 = Q_\eta^2 + (x_o \mp Q_\eta)^2 + 2Q_\eta(x_o \mp Q_\eta)\cos\varphi \tag{21}$$

and

$$r_\xi = -Q_\eta - (x_o \mp Q)\eta\cos\varphi, \tag{22}$$

where $\varphi$ represents the angle which the normal to the zero-velocity curve at any point near A or B makes with the positive $x$-axis. When two signs appear together, the upper one corresponds to point A and its neighborhood and the lower one points to B and its neighborhood. Again $\eta = -\varphi$ as in the first case of asymptotic expansions. With the aid of equations (21) and (22) we may reduce equation (14) to

$$u_\eta^2 - 2Q_\eta u\eta + kQ_\eta^2 = o \tag{23}$$

where

$$k = \frac{\mu(1-\mu)}{x_o \mp Q_\eta}\left(\frac{1}{r_1^3} - \frac{1}{r_2^3}\right) \tag{24}$$

for point A and B respectively according to whether we take the upper or lower sign in equation (24). The solution of equation (23) is

$$u_\eta = Q_\eta[1 - (1-k)^{\frac{1}{2}}], \tag{25}$$

the minus sign before the parenthesis has been chosen in order to agree with the asymptotic behavior found previously in equation (18). The radius of curvature $Q_\eta$ can be derived from equation (9). We shall omit its long expression here.

We have computed $u_\eta$ according to equation (25) for several cases of $x_o$ with $\mu = 0.2$. It appears evident from the results of computations that velocities thus obtained are very near to those found in the periodic orbits which we may obtain either by the numerical process of successive approximation (Huang and Wade 1963) or by the series solution (Huang 1964). In the second and third column of Table 1 we have a few velocities of a particle as it crosses the $x$-axis obtained by equation (25) and from the periodic solutions respectively. Needless to say, the disagreement in sign between $\dot{y}$ and $u_\eta$ in one half of

the cases in Table 1 arises purely from the difference in the coordinate system. We should compare only the magnitudes between the second and third column. As would be expected, the agreement between two kinds of computations becomes better and better as we approach more and more to the star. Thus, the gaseous rings found observationally in many binary systems may be regarded equivalently either as a hydrodynamic flow or as motions of particles in a continuous series of periodic orbits that exist around the component.

TABLE 1.—*A Comparison of Velocities at Points on the x-axis Obtained from Equation (14) and from Periodic Solutions*

| $x_0$ | $u$, From Eq. (14) | $\dot{y}$ From Periodic Solutions |
|---|---|---|
| .054472 | −1.492 | 1.525 |
| −.450000 | −1.529 | −1.556 |
| .001841 | −1.775 | 1.791 |
| −.400000 | −1.794 | −1.809 |
| −.049380 | −2.148 | 2.154 |
| −.350000 | −2.156 | −2.164 |
| −.099858 | −2.724 | 2.726 |
| −.300000 | −2.727 | −2.730 |
| −.149986 | −3.949 | 3.949 |
| −.250000 | −3.950 | −3.950 |

## V. THE FORBIDDEN ZONE

Since our approach to the problem of gaseous flow in the binary system emphasizes the two phvsical quantities $C$ and $h$, it is interesting to point out that at some points in space, a certain combination of values for these two quantities is incompatible. In other words, with a given value of $C$ and $h$, sometimes the particle cannot into a certain region of space which we shall call the forbidden zone. It can be easily seen as follows. We may express equations (1) and (5) simply as

$$\dot{x}^2+\dot{y}^2+\dot{z}^2 A, \tag{26}$$

and

$$x\dot{y}-y\dot{x}=B, \tag{27}$$

where $A$ and $B$ are functions of $x$, $y$, $z$, $C$ and $h$ and can be easily found from equations (1) and (5). Now in the $(x, y, z)$ velocity space, equation (26) represents a sphere with the center at the origin and with a radius equal to $A^{1/2}$, while equation (27) represents a plane. It is then obvious that for any given combination of $A$, $B$, $x$, $y$, $z$ (or equivalently $C$, $h$, $x$, $y$, $z$) the two surfaces may or may not intersect with each other. If they do not, no real velocity components $(x, y, z)$ will satisfy both equations. This means that the particle with the given values of $C$ and $h$ cannot reach the point $(x, y, z)$. In other words, the point $(x, y, z)$ lies in the forbidden zone associated with the given $C$ and $h$ values.

The forbidden zone can be easily calculated from the condition that the distance of the origin from the plane given by equation (27) in the velocity place is greater than the radius, $A^{1/2}$ of equation (26). Explicitly, the forbidden zone is given by

$$B^2>A(x^2+y^2) \tag{28}$$

We shall illustrate the forbidden zone only in the $x$, $y$ plane. It can be obtained by plotting the curve defined by the following equation

$$f(r, \theta)\equiv r^2+r\left[r^2+\frac{2(1-\mu)}{r_1}+\frac{2\mu}{r_2}-C\right]-h=0. \tag{29}$$

where $\theta$ which enters into the expression for $r_1$ and $r_2$ denotes the angle between the radius vector $\vec{r}$ of the third body and the positive $x$-axis.

Although $h$ is a physical quantity, it is not a constant of motion in the restricted three-body problem. Consequently, the forbidden zone is not as important as the zero-velocity curves in depicting the motion of particles. However, combined with the property of $dh/dt$ discussed in the previous section, the forbidden zone may serve some useful purpose of excluding certain modes of gaseous flow in the binary system.

Figure 1 illustrates three forbidden zones in the $x$, $y$ plane for $C=3.5$ and for the three values of $h$. The areas that include the origin are forbidden to particles having the assumed $C$ and $h$ values. Because of the symmetry with respect to the $x$-axis, only one half of the zone is drawn in each case. However, the signs of $dh/dt$ are marked in the figure in all four quadrants at the corners.

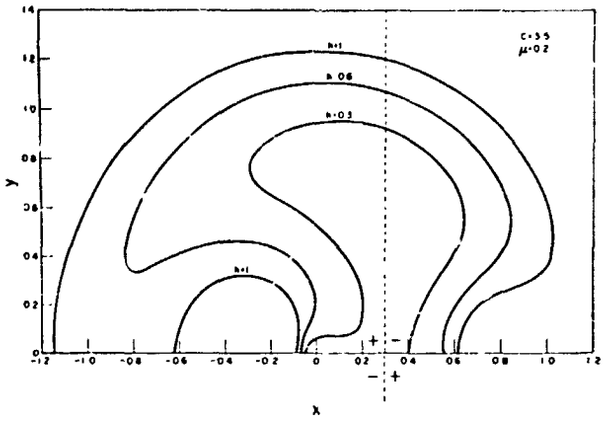

FIGURE 1.—The Forbidden Zone—Particles with given $C$ and $h$ at any instant cannot be found in a certain region of space, called the forbidden zone. Three forbidden zones in the $xy$ plane are illustrated here for three pairs of $(C, h)$. They are (3.5, 1), (3.5, 0.6) and (3.5, 0.3). Because of symmetry with respect to the $x$-axis, only one-half of each zone is shown here. The forbidden zone corresponding to each of the other two pairs of $(C, h)$ lies inside a single closed curve. The sign of dh/dt is marked at each corner of the four quadrants formed by $x=o$ and $y=0.5$.

## VI. SOME REMARKS CONCERNING THE ROTATING GASEOUS RINGS OBSERVED IN THE BINARY SYSTEM

### 1. The Chance of Ring Formation

Let us denote $C_1$ and $C_2$ as the value of $C$ that corresponds respectively to the innermost and outermost contact surface (Kuiper, 1941). The latter will be hereafter called, for the sake of brevity, the $S_1$ and $S_2$ surface. Both $C_1$ and $C_2$ have been computed by Kopal (e.g. 1959) and Kuiper and Johnson (1956).

According to the result obtained in the restricted three-body problem, those ejected particles whose C values are greater than $C_1$ cannot penetrate the $S_1$ surface, and those whose $C$ values are greater than $C_2$ cannot penetrate the $S_2$ surface. It follows that those particles whose $C$ values are less than $C_2$ could escape from the system and those whose $C$ values are larger than $C_1$ will remain inside the $S_1$ surface.

The quantity,

$$\Delta C = C_1 - C_2, \tag{30}$$

measures the closeness of the two critical zero-velocity surfaces $S_1$ and $S_2$ and may have an important effect on the flow of matter ejected by the secondary component into the primary lobe of the $S_1$ surface. We do not mean that only those particles with $C$ values between $C_1$ and $C_2$ will penetrate into this volume, since any particle with $C<C_1$ can move into it. But the amount of accumulation of matter inside this volume at any given time perhaps increases with the increase of $\Delta C$. It follows from this reasoning that formation of gaseous rings around the primary $(1-\mu)$ component favors large values of $\mu$, as we can easily see, for example, from Kuiper and Johnson's Table, that $\Delta C$ increases with $\mu$.

On the other hand, we have pointed out (Huang and Struve, 1956) that from the consideration of available space for their ring formation around primary component, gaseous rings have a better chance to exist in binaries of small $\mu$. From the two arguments we may conclude that perhaps formation of gaseous rings has its highest chance in binaries with $\mu$ neither near the maximum end of 0.5 nor near the minimum end of approaching zero. Observationally gaseous rings have been found in binaries with $\mu$ around 0.2. While this result agrees with the prediction from the previous simple arguments, it may also be caused by the effect of observational selection, since it is extremely difficult to measure $\mu$ when it is much less than 0.1

In passing, it may be noted that following the argument of available space we have predicted a few eclipsing binaries in which gaseous ring may be expected but not yet observationally detected (Huang and Struve, 1956). Among these predicted stars is $\beta$ Per. (Algol) whose emission feature was later discovered by Struve and Sahade, 1957. While they have concluded that the emission feature does not indicate a ring structure, it nevertheless reveals an accumulation of gases in the system. And the accumulation of gases is a necessary condition for the ring formation.

### 2. Ring Formation, Mass Dissipation and Ejection Velocities

It is evident from observations that the gaseous particles flowing in the binary system come from the component stars themselves (e.g. Wood 1950; Kopal 1959; Sahade 1960). In fact, it is usually the less massive component that is losing mass. Accordingly, we will assume the injection of particles into the system by the $\mu$ component.

Let $\vec{V}$ be the velocity of ejection with respect to that point of the stellar surface from which the

particle is ejected. If the secondary component is rotating axially as a rigid body with an angular velocity $\vec{\omega}$ with respect to a stationary frame of reference, any particle that is attached to the surface rotates with a velocity $\vec{\omega}\times\vec{R}_2$ where $\vec{R}_2$ is the radius vector of a point on the secondary surface from its center. Since the center of the secondary revolves with a unit angular velocity $\vec{k}$ in the $z$-direction in its orbit, the ejection velocity in the $xyz$ coordinate system is given by

$$\frac{d\vec{r}}{dt}=\vec{V}+(\vec{\omega}-\vec{k})\times\vec{R}_2. \tag{31}$$

In order to compute the $C$ values of ejected particles, we can take advantage of the fact that the surface of the secondary coincides with the secondary lobe of the $S_1$ surface. Thus, it follows from the equation (1) that

$$C-C_1-\left(\frac{d\vec{r}}{dt}\right)^2 \tag{32}$$

If axial rotation and orbital revolution of the secondary ($\mu$) component are synchronized

$$C=C_1-V^2.$$

While the particles ejected from the secondary component has values always less than $C_1$ according to equation (32), the $C$ values corresponding to those periodic orbits close to the $1-\mu$ component are greater than $C_1$. It becomes evident that before the ejected particles accumulate to form gaseous rings close to the primary component, they must have collided one another many times such that $C$'s of some particles have been increased to the necessary values to make the ring formation possible. Because of the conservation law given by equation (3) we may expect that $C$'s of other particles must have been reduced as a result of collisions. Since particles of small $C$ correspond to high velocities, they will easily escape from the system. It can, therefore, be concluded that the formation of gaseous rings of small radii around the primary component must be accompanied by dissipation of mass from the system.

If $V$ should be very large, it would be doubtful whether the velocities of an appreciable amount of particles can be reduced by collisions to make ring formation possible. Therefore, we would suggest that the ejection velocities from the secondary are in general, small if gaseous rings are observed around the primary component. That is why we have classified ejection leading to the ring formation as a slow mode (Huang 1963).

### 3. Evolution and Physical Significance of Rotating Gaseous Rings

The gaseous rings around the primary component formed by the material from the secondary component cannot be permanent. Because of the tidal friction, the rapidly rotating ring will gradually lose the angular momentum to its original source of orbital motion. As the angular momentum of rotating particles decreases, they fall into the primary. Therefore, without other disturbances, the rotating rings represent only an intermediate step in the transfer of mass from the secondary to the primary component. If the ring will be dissipated easily, its presence can only indicate an active secondary at the epoch of observation.

We know solar surface activities because they provide us with a disk to observe. In the case of stars, little can be learned about their surface conditions because they appear to us as point sources, although eclipsing binaries have revealed some of the secrets of the stellar surface. Now from the observable behavior of gaseous rings we can derive, according to the present idea of ring formation, the mode of ejection of mass from stellar surface. Thus, if the ring can maintain its existence only when matter is continually supplied to it by the secondary component, its fluctuations in intensity or even its disappearance and re-emergence, which have been actually observed (Wyse 1934; Joy 1947; McNamara 1951) can only reflect the manner in which matter from the secondary is ejected.

Rings may disappear when the secondary ceases to eject matter. In this case, their disappearance would be gradual. Rings may also disappear when the secondary suddenly ejects a large number of particles of high velocities. The latter simply sweeps all rotating particles off their orbit. In this case, the disappearance of rings would most likely occur suddenly. Perhaps the fluctuation of light intensity of gaseous rings and sometimes their total disappearance actually observed are due to the second cause.

In any case, from what has been observed of the gaseous rings the ejection of matter from the

stellar surface does not resemble a continuous steady process such as the evaporation from a liquid surface. If there is ever a steady background flow out of the secondary, it is superimposed by intermittent bursts like the prominence activities on the solar surface. Thus, by observing the variation in intensity and structure of the emission lines that are produced by the rotating rings we will be able to learn something about the manner of how a component star loses its mass when its evolutionary stage of expansion brings it to touch the $S_1$ surface. Since such an empirical knowledge is unlikely to be found elsewhere, the importance of observing gaseous emission in binary systems cannot be exaggerated.

There remains the question whether a rotating ring or disk can be formed around the secondary (less massive) component when the primary component is losing mass. It is obvious that the ring would be less stable around the secondary than around the primary because of a larger perturbation in the first case. Also the available volume for ring formation is smaller in the first than the second case. But there is no a priori reason to believe that rings cannot be formed around the secondary component. However, observationally we have never found a gaseous ring around the secondary component.

Actually we have found few binaries whose more massive component has filled the primary lobe of the $S_1$ surface while those of less massive components remain small compared with the secondary lobe of the $S_1$ surface. Therefore, the impending question is not why we have not found any gaseous ring around the less massive component, but rather why systems whose more massive component injects particles into the secondary lobe should be so rare. Presumably, some selection effect plays a role here, but it is unlikely that this is the sole cause.

## ACKNOWLEDGMENT

It is my pleasure to note my sincere thanks to Mr. Clarence Wade, Jr. for performing on the IBM 7094 computer some numerical calculations involved in this paper.

## REFERENCES

BROUWER, D. and CLEMENCE, G. M., 1961, "Methods of Celestial Mechanics," Variation of Parameters, Chap. 11, New York Academic Press.
GOULD, N. L., 1959, A. J., **64**, 136.
HUANG, S. -S., 1963, Ap. J., **138**, 471.
HUANG, S. -S., 196x, to be published.
HUANG, S. -S. and STRUVE, O., 1956, A.J., **61**, 300.
HUANG, S. -S. and WADE, C., JR., 1963, A. J., **68**, 388.
JOY, A. H., 1942, Pub. A.S.P., **54**, 35.
JOY, A. H., 1947, Pub. A.S.P., **59**, 171.
KOPAL, Z., 1959, "Close Binary Systems," London: Chapman and Hall.
KUIPER, G. P., 1941, Ap. J., **93**, 133.
KUIPER, G. P. and JOHNSON, J. R., 1956, Ap. J., **123**, 90.
MCNAMARA, D. H., 1951, Ap. J., **114**, 513.
MOULTON, F. R., 1914, "An Introduction to Celestial Mechanics" 2nd Ed., New York: Macmillan, Chap. 8.
PRENDERGAST, K. H., 1960, Ap. J., **132**, 162.
SAHADE, J., 1960, "Stellar Atmospheres" Ed. J. L. Greenstein, Chicago: University of Chicago Press, Chap. 12.
STRUVE, O., 1950, "Stellar Evolution," Princeton: Princeton University Press.
STRUVE, O. and JAHADE, J., 1957, Pub. A.S.P. **69**, 41.
WOOD, F. B., 1950, Ap. J., **112**, 196.
WYSE, A. B., 1934, Lick Obs. Bull. **17**, 37 (No. 464).

# APPENDIX

## DERIVATION OF EQUATIONS (7)–(8) FROM HYDRODYNAMIC CONSIDERATIONS

Equation (7) has been derived already by Prendergast (1960), while equation (8) can be obtained as follows: if we neglect the pressure term, the hydrodynamic equations in the orbital $x$–$y$ plane become:

$$\frac{\partial u_x}{\partial t}+u_x\frac{\partial u_x}{\partial x}+u_y\frac{\partial u_x}{\partial y}-2\mu_y=\frac{\partial U}{\partial x} \tag{1}$$

$$\frac{\partial u_y}{\partial t}+u_x\frac{\partial u_y}{\partial x}+u_y\frac{\partial u_y}{\partial y}+2u_x=\frac{\partial U}{\partial y} \tag{2}$$

Multiplying equation (1) by $y$ and equation (2) by $x$ and subtracting the two resulting equations we obtain

$$x\frac{\partial u_y}{\partial t}+x\left(u_x\frac{\partial u_y}{\partial x}+u_y\frac{\partial u_y}{\partial y}\right)+2xu_x-y\frac{\partial u_x}{\partial t}-y\left(u_x\frac{\partial u_x}{\partial x}+u_y\frac{\partial u_x}{\partial y}\right)+2yu_y=x\frac{\partial U}{\partial y}-y\frac{\partial U}{\partial x} \tag{3}$$

Since $h$ may be written now as

$$h=x^2+y^2+xu_y-yu_x, \tag{4}$$

it can be easily shown that equation (3) becomes identical to equation (8) in the main test.

# ROTATIONAL BEHAVIOR OF THE MAIN-SEQUENCE STARS AND ITS PLAUSIBLE CONSEQUENCES CONCERNING FORMATION OF PLANETARY SYSTEMS*

SU-SHU HUANG†

A phenomenological theory for the behavior of axial rotation of main-sequence stars is proposed here by considering the effect of braking. It does not specify the physical process of braking but does provide a statistical model by which histograms of observed rotational velocities of stars of different spectral types can be explained in terms of the braking strength. It shows that rotation of all stars including those of O and B type has been braked in various degrees during their course of evolution.

As a result of braking, the stellar angular momentum is transferred outwards to the surrounding nebula that may be regarded as the remnant of star formation. This leads plausibly to the formation around the star of a planetary system from the nebula. If the angular momentum is not further dissipated from the nebula, we can estimate the size of the planetary system and its probability of occurrence. It shows that the size of a planetary system around any star is critically dependent upon the mass in the nebula as compared to that of the star itself.

## I. A THEORY FOR EXPLAINING THE OBSERVED DISTRIBUTION OF STELLAR ROTATIONAL VELOCITIES

Axial rotation of the main-sequence stars stops quite abruptly at about F5 (Struve 1930). It has frequently been attributed to the braking effect of various mechanisms reviewed in a previous paper (Huang and Struve 1960). A more efficient braking mechanism than those previously proposed has recently been suggested by Schatzman (1962) as due to mass loss through stellar magnetic activities.

In the present paper we do not intend to discuss the physical process of how the braking of stellar rotation is actually affected. Rather, we will show phenomenologically that the observed distribution of rotational velocities of stars belonging to different spectral types can indeed be understood in terms of braking strengths.

As the result of a statistical study (Struve 1945; Huang and Struve 1954) it has been concluded that the rotational axes show no preference in their directions in space. This indicates that the rotating stars have not acquired their angular momentum from the galactic rotation of the pre-stellar gaseous medium. Instead, their angular momenta must have been derived from a random process, such as collisions of interstellar clouds, turbulence, etc. (Huang and Struve 1954). Consequently, we may expect that the angular momenta per unit mass, $h$, of stars are originally distributed according to the Maxwellian law. Finally we would like to call attention here to the fact that this observational consequence has not been fully appreciated. Many theoreticians still take the rotational angular momenta of stars as due ultimately to the galactic rotation of the tenuous pre-stellar medium (e.g. Edgeworth 1946; Hoyle 1960).

For a given spectral type the geometrical radius and the radius of gyration do not vary greatly. Hence, we may take the equatorial rotational velocity, $v$, to be in direct proportion to $h$. If we set $x = v/v_m$, where $v_m$ denotes the most probable

*Published in The Astrophysical Journal 141: 985, April 1965.

†Goddard Space Flight Center and Catholic University, Washington, D. C.

equatorial rotational velocity, the original distribution of $x$ in a given spectral range should be given by

$$f_o(x) = \frac{4\gamma}{\sqrt{\pi}} x^2 e^{-x^2}, \quad x \leq x_c \tag{1}$$

according to our assumption. Here $x_c$ is the upper limit of rotational velocities because of rotational instability and $\gamma$ is a numerical factor to normalize the function $f_o(x)$. Now if we assume that the star rotates as a rigid body, $x$ is obviously related to the angular momentum per unit mass, $h$, of the star as follows:

$$h = Rk^2 v_m x \tag{2}$$

where $R$ is the geometrical radius and $Rk$ the radius of gyration of the star. We may define $h = h_c$ by equation (2) when $x = x_c$. Then interstellar clouds with $h > h_c$ could very possibly lead to the formation of close binary systems. Since at present we are interested mainly in the behavior of the observed distribution at its small-velocity end which is not significantly affected by the high-velocity tail, we shall set, for simplicity of calculation, $x_c > \infty$ and consequently $\gamma = 1$.

As a simple model, we propose that the effect of braking is to reduce $h$ of all stars in a given spectral range by a constant amount, $h_1$. Define $x = x_1$ when $h = h_1$ is substituted in equation (2). It is then obvious that $x_1$ measures the degree of braking of axial rotation of the stars within a spectral type, namely, the stronger the braking mechanism, the greater the value of $x_1$. In this way we are able to obtain the distribution of rotational velocities after the braking mechanism has been applied.

Needless to say, this statistical model is very idealized and represents an extreme case. Most likely $h_1$ is not a constant even within a spectral sub-type but increases with the original value of $h$. However, since the observed distribution is not well determined, we do not see any advantage at this moment to build an elaborate model which usually would involve many adjustable parameters. On the other hand, because of this over-simplified model, the quantitative results obtained in this paper represent only a very rough estimate.

If we accept this simplified model, the distribution of equatorial rotational velocities after braking has taken its toll becomes

$$f(x, x_1) = \psi_o(x_1)\delta(x-o) + \frac{4}{\sqrt{\pi}}(x+x_1)^2 e^{-(x+x_1)^2} \tag{3}$$

where

$$\psi(x) = \frac{2}{\sqrt{\pi}}\left(\int_o^x e^{-t^2} dt - x e^{-x^2}\right) \tag{4}$$

and $\delta(x-o)$ denotes the delta function.

If $\varphi(y, x_1)$ denotes the distribution of observed velocities, $y$, we have (Kuiper 1935; Chandrasekhar and Münch 1950)

$$\varphi(y, x_1) = y \int_y^\infty \frac{f(x, x_1)dx}{x(x^2-y^2)^{\frac{1}{2}}} \tag{5}$$

Substituting equation (3) into equation (5) we obtain

$$\varphi(y, x_1) = \psi_o(x_1).\delta(y-o) + \psi(y, x_1) \tag{6}$$

where

$$\psi(y, x_1) = \frac{4}{\sqrt{\pi}} \int_o^{\pi/2} (y \sec\theta + x_1)^2 e^{-(y \sec\theta + x_1)^2} d\theta \tag{7}$$

The observed distributions are given in the form of histograms, i.e.,

$$\Phi(y, x_1) = \int_{(n-1)\Delta y}^{n\Delta y} \varphi(y, x_1)dy, \qquad \gamma(n-1)\Delta y < y < n\Delta y. \tag{8}$$

In Figure 1 we have shown 11 computed histograms of $\Phi(y, x_1)$ according to equations (5)–(7) for / / values of $x_1$ (0, 0.1, 0.2, 0.3, 0.4, 0.5, 0.6, 1.0, 1.4, 1.8, 2.6) with $\Delta y = 0.2$. This sequence of histograms illustrates the effect of the braking strength on the distribution of observed rotational velocities of stars in a spectral type. The case $x_1 = 0$ corresponds to that of no braking, while the case $x_1 = 2.6$ leads practically to a complete stop of axial rotation by braking.

These diagrams should be compared with the observed histograms. Unfortunately, as we can see in our previous paper (Huang 1953), the two sets of observed diagrams derived from two uncombinable sets of observational data show slight differences. The two uncombinable sets of observational data are respectively from the three-prism and two-prism spectrograms that have

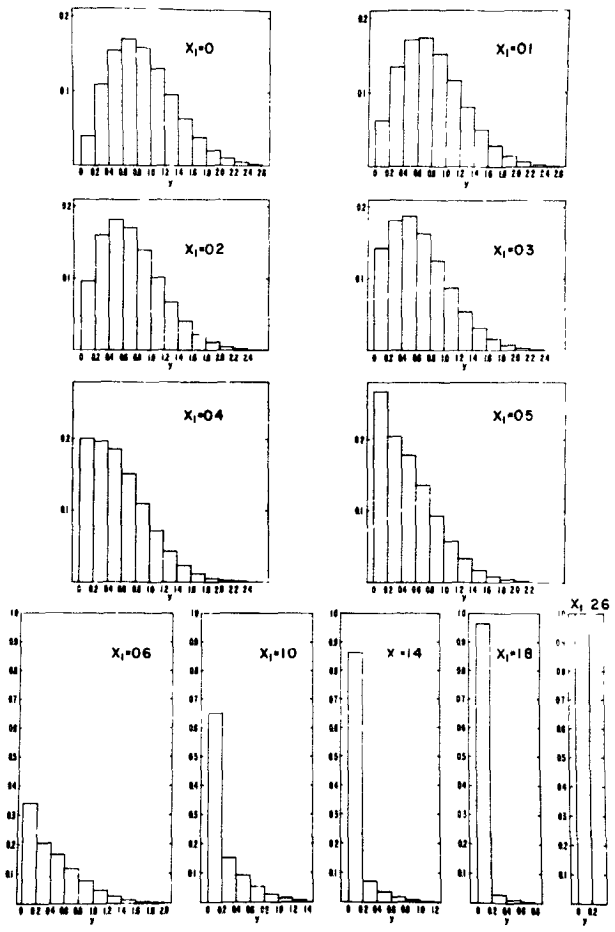


FIGURE 1.—Computed histograms of projected rotational velocities of groups of stars that have suffered different degrees of braking. We have plotted here 11 histograms for 11 values of $X$, which, according to our model, measures the strength of braking of stellar axial rotation.

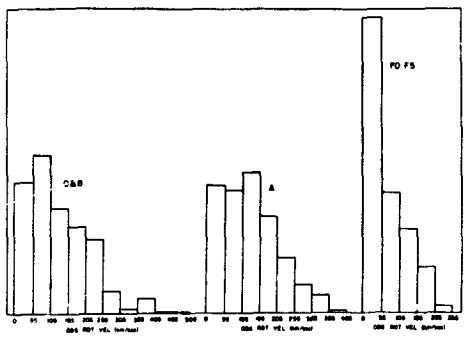


FIGURE 2—.Observed histograms of projected rotational velocities of three groups of stars, O and B, A and F0–F5, taken from a previous paper. The histogram of projected rotational velocities for later type stars will be consisted of only a single column of small velocities. These histograms should be compared with those in Figure 1. The trend of increasing braking strengths from O and B, through A and F0–F5 to later-type stars is unmistakable. From the comparison we may make a rough estimate of $x_1$ for each of these three groups of stars.

been taken during the years by astronomers at the Lick Observatory. There are 1103 stars for which rotational velocities were measured from three-prism spectrograms and 445 stars for which rotational velocities were measured from two-prism spectrograms. Therefore, the histograms of rotational velocities derived from the three-prism spectrograms are definitely more reliable than those from the two-prism spectrograms from a consideration of both the dispersion and the number of stars studied. For this reason we shall compare the computed histograms in Figure 1 with the observed ones obtained from three-prism histograms, the latter being reproduced here in Figure 2. Finally, it may be noted that there are available better observational data for rotational velocities (Slettebak 1949 et seq.; Cf. Huang and Struve 1960) than what was adopted here. However, our crude measurements of stellar rotational velocities provide the only uniform set of data which cover such a large number of stars that make the histograms in Figure 2 statistically significant.

In Table 1 we give the results of our determination of $x_1$ and $v_m$ for each of three observed histograms after a comparison with those in Figure 1, $x_1$ being determined by the shape and $v_m$ by the scales of abscissas of both observed and computed diagrams. It should once more be emphasized that these values are very tentative as both theory and observational data (especially the conversion of measured widths of the spectral line to rotational velocities) are crude. However, there is no doubt at all that $x_1$ is least (but definitely non-vanishing) for O and B-type stars, increases only slightly for A-type stars and becomes much larger for F0–F5 stars. Since few single stars of spectral types later than F5 are found to be rotating with a measurable velocity, we must conclude that $x_1$ for these late-type stars is greater than 2.6.

While we cannot determine $x_1$ accurately because of the uncertainty in observational data, the general behavior does indicate that our simple statistical model for the braking effect represents very well the gradual change of the distribution of observed rotational velocities from O and B through A and F0–F5, and finally to later-type

stars. Especially it explains the long puzzled fact that a large number of O, B, A stars do not rotate appreciably, although their average rotational velocities as group are high.

The previous result induces us to conclude that contrary to our previous belief, braking is not limited only to stars of spectral types later than F5 but extends to O, B, A and early F stars as well. It suggests that along the main sequence all stars show evidence of having been braked. However, the braking mechanism is weak at the upper branch of the main sequence and increases its strength rapidly after F0. It becomes so strong after F5 that rotation of all stars is practically stopped by it.

We have mentioned before that by assuming $x_c \to \infty$ we introduce an approximation. While this approximation does not seriously modify the distribution function at the lower end of observed rotational velocities, it makes an appreciable difference at the upper end. Thus, when we compare histograms (those of $x_1 = 0.3$, 0.4 and 0.8) in Figure 1 with those in Figure 2, we can immediately see a systematic difference arising from this approximation, since in all three histograms obtained from observed data, the distribution function drops much more rapidly than what have been calculated on the assumption of $x_1 \to \infty$. Thus, a cut-off of rotational velocities at their upper end is evident in all three cases in Figure 2. This shows that rotational instability has played a role not only in O- and B-type stars but also in F- and perhaps even later-type stars sometime during the course of their evolution. This result may be significant to our search of clues for star formation.

The strength of braking varies with the moment of braking force and the duration in which braking acts. If indeed the braking is due to magnetic activities which are in turn induced by convection and rotation itself in the early phase of the star's evolution as Schatzman (1962) has suggested, we would expect from the present study that magnetic activities have occurred in stars of all masses in their early phases of evolution, differing only in the strength and duration of such activities. This conclusion is in agreement with Pvoeda's (1964) interpretation of flare stars based on Hayashi's (1961) results of evolution on one hand and Fowler, Greenstein and Hoyle's (1962) theory of formation of light elements—Li, Be, B—in the early phase of the solar system on the other.

Thus far, we have followed the reasoning of both Schatzman and Poveda that the magnetic field is generated in the star as a result of convective motion and differential rotation. However, it may be noted that it would not modify our conclusion if we assume that the strong magnetic field is derived from accretion of interstellar magnetic lines of force during the period of star formation. If so, the strong magnetic activities in the early phase would represent the dissipation because of convection, of magnetic energy that is already there.

## II. PROBABILITY OF FORMATION OF PLANETARY SYSTEMS AROUND STARS

It has often been suggested (e.g. Huang 1959) that the disappearance of rotation after F5 may indicate the emergence of planetary systems because it is difficult to understand how the original distribution of angular momenta of the late-type stars should be so radically different from that of early ones. This is especially true if we follow the reasoning in the previous section where the original distribution of angular momenta per unit mass of stars is assumed to follow the Maxwellian distribution (which may be truncated at the high-value end because of rotational instability). Indeed, if angular momenta that have been dissipated from the stars remain in their neighborhood, formation of planetary systems would appear inevitable. Following this line of reasoning we shall make in this section an estimate, though a very crude one, not only of the probability among single stars that will possess planetary systems but also of their general behavior with respect to the spectral type of their parent stars.

Before we shall understand why our planetary system was formed in a state as it is, we are not expected to derive, simply from a consideration of the angular momentum, the detailed structure of planetary systems around stars. In order to obtain a general behavior of any planetary system around a star without going into the detail structure we may define the concept of an "equivalent planet," which is a fictitious planet that would be moving in a circular orbit with an angular momentum per unit mass, $h'$, equal to the average value

of the entire mass outside of, but belonging to, the star. Thus, in the case of our solar system, we have (Allen 1955) the total angular momentum of the planetary system equal to 3.15 x $10^{50}$ gm cm$^2$/sec, while its total mass is 2.68 x $10^{30}$ gm. Consequently, its $h'$, denoted hereafter by $h_s'$ is

$$h_s = 1.176 \times 10^{20} \text{ cm}^2/\text{sec}. \tag{9}$$

Then it is easy to find that the equivalent planet of our own planetary system is located at a distance

$$a_s = 1.042 \times 10^{14} \text{ cm} \tag{.10}$$

from the sun (i.e. between Jupiter and Saturn as would be expected) and revolves with a linear velocity

$$V_s = 11.3 \text{ } km/\text{sec}. \tag{11}$$

around the sun. It is obvious from our definition of the equivalent planet that it does give us a measure of the extent of any planetary system although it conveys no idea about its total mass and mass distribution in the system.

Let us now assume that the gaseous remnant around a star after its formation is $m$ and the mass, radius and radius of gyration of the star itself are respectively $M$, $R$, and $Rk$. Therefore, the total angular momentum of the star is

$$\Omega(v) = MRk^2v \tag{12}$$

After braking, all of its angular momentum is transported into the surrounding medium (of mass $m$) according to our theory if $v \leq v_1 (= x_1 v_m)$ and a constant part (equal to $\Omega_1 = MRk^2 v_m x_1$ of it is transported out if $v > v_1$. However, we should realize that the angular momentum in the nebula that will evolve to become a planetary system could be different from what has been fed into it by the star, because some angular momentum, say $\vec{\Omega}_0$, may be originally associated with it and has never gone into the star. Since both the star and its surrounding nebula are supposed to have been formed from the same interstellar medium, we may reasonably assume that the vector, $\vec{\Omega}_0$, points to the same direction as the stellar angular momentum does. Hence, we can consider their magnitudes only and the angular momentum associated with the nebula (of mass $m$) after the completion of braking process has the following value:

$$\begin{aligned} \Omega(x) &= MRk^2 v_m x + \Omega_0 \text{ for stars with } x \leq x_1 \\ &= MRk^2 v_m x_1 + \Omega_0 \equiv \Omega_1 \text{ for stars with } x > x_1 \end{aligned} \tag{13}$$

For stars with slow rotation which indicates smallness of $h$ of the pre-stellar medium, $\Omega_0$ must be small and may be neglected. However, for stars of rapid rotation and especially for those which have passed through the stage of rotational instability in the course of their evolution, $h$ of the prestellar medium must be large and $\Omega_0$ large too.

If we include the possibility that a part of the angular momentum in the nebula may be dissipated away (for example through the loss of mass), $\Omega_0$ may be even negative. Thus, $\Omega_0$ cannot be estimated from the present consideration. However, as we shall see, this uncertainty can be formally circumvented in the following calculation.

Since

$$h' = \frac{\Omega}{m} = (GMa)^{\frac{1}{2}}, \tag{14}$$

where $a$ is the radius of the equivalent planet's orbit around a star and

$$h_s' = a_s V_s = (GM_\odot a_s)^{\frac{1}{2}} \tag{15}$$

for the planetary system of the sun, we may introduce a new variable

$$\xi = \left(\frac{Ma}{M_\odot a_s}\right)^{\frac{1}{2}} \tag{16}$$

to measure the size of the equivalent planet's orbit around any star. It follows from equations (13)–(16) that $\xi$ extends from

$$\xi_0 = \frac{\Omega_0}{ma_s V_s} \quad \text{to} \quad \xi_1 = \frac{\Omega_1}{ma_s V_s} \tag{17}$$

if $\Omega_0$ is positive and zero to $\xi_1$, if $\Omega_0$ is negative. Therefore, the lower and upper limit of the radius of the equivalent planet's orbit denoted respectively by $a_0$ and $a_1$ are given by

$$\xi_0 = \left(\frac{Ma_0}{M_\odot a_s}\right)^{\frac{1}{2}} \quad \text{and} \quad \xi_1 = \left(\frac{Ma_1}{M_\odot a_s}\right)^{\frac{1}{2}} \tag{18}$$

Now $x$ and $\xi$ are related by

$$x=\lambda\xi-\frac{\Omega_o}{MRk^2v_m} \tag{19}$$

where

$$\lambda=\frac{m}{M}\frac{a_s}{R}\frac{V_s}{v_m}\frac{1}{k^2} \tag{20}$$

It is easy to derive from equations (1) and (19) that the distribution function $\delta(\xi)$ with respect to $\xi$.

If we further let

$$t=\xi-\frac{\Omega_o}{ma_sV_s} \tag{21}$$

and

$$t_1=\xi_1-\frac{\Omega_o}{ma_sV_s}=\frac{x_1}{\lambda} \tag{22}$$

we obtain from $\delta(\xi)$ that

$$g\left(t+\frac{\Omega_o}{ma_sV_s}\right)=\frac{4}{\sqrt{\pi}}\lambda^3t^2e^{-\lambda^2t^2}\delta(t-t_1)[1-\psi_o(x_1)] \tag{23}$$

Since from $t$ to $\xi$ it involves only a horizontal translation, the shape of the distribution function does not depend upon $\Omega_0$. If $\Omega_0$ is positive, we simply translate the entire curve to the right, thereby increasing systematically the size of the expected orbits. If $\Omega_0$ is negative, we translate the curve to the left and set the probability to zero everywhere that is on the left side of the origin. In this way we are able *formally* to take into account any value of $\Omega_0$. Physically, however, we should remember that $\Omega_0$ likely varies from case to case and moreover we do not know how it does vary (say, with respect to $M$, $h$, $m$, $h^1$, etc.). Hence, it is one of the uncertain factors that prevent us to derive the probability of occurrence of a planetary system of a given size.

Since we can obtain easily the distribution with respect to $\xi$ from that with respect to $t$, we shall consider hereafter only the latter which, as we see from equation (24), depends upon two parameters, $\lambda$ and $t^1$ or equivalently $\lambda$ and $x$, because of equation (23). While $x_1$ has been determined from observed data, $t$, involves an unknown parameter, namely $m/M$.

From the values of $x_1$ and $v_m$ in Table 1 we can compute $t_1$ (or $\lambda$) for each of the three cases given there. We shall use the mean radius $R/R_\odot=3.9$ and mean mass $M/M_\odot=5.9$ for O and B stars, $R/R_\odot=1.74$ and $M/M_\odot=2$ for A stars and $R/R_\odot=1.35$ and $M/M_\odot=1.4$ for F0–F5 stars. In all cases we adapt $k^2=0.05$. Then it follows from Table 1 and equations (20) and (23) that $mt_1/M$

TABLE 1.—*Values of $x_1$ and $v_m$ determined from a Comparison and Observed and Calculated Histograms of Rotational Velocities*

| Sp. Type | $x_1$ | $v_m$(km/sec) |
|---|---|---|
| O and B | 0.3 | ~200 |
| A | 0.4 | ~200 |
| F0–F5 | 0.8 | ~200 |
| later than F5 | >-2.6 | ---------- |

is equal to $6.9\times10^{-4}$ for O and B stars, equal to $4.1\times10^{-4}$ for A stars, and equal to $6.4\times10^{-4}$ for F0–F5 stars. It is quite evident that the error involved in the determination of $x_1$ and $v_m$ is much greater than the differences we have found in these three expressions of $t_1$. Consequently, we may roughly set

$$t_1=6\times10^{-4}\frac{M}{m} \tag{24}$$

as representing all stars from 0 to F5. If $=0$, equation (24), when combined with equations (17), (18) and (23), gives

$$\frac{a_1}{a_s}=(6\times10^{-4})^2\frac{MM_\odot}{m^2} \tag{25}$$

which states that the maximum size of the planetary system is directly proportional to the mass of its parent star and inversely proportional to the square of its total mass. It should be noted that the numerical coefficient in equation (24) does not apply to stars later than F5 for which we do not have any observed data for making the calculation.

We have seen how critically does the size of a planetary system depend upon the mass in the

nebula. A further complication is the dissipation of mass in the nebula and accompanying dissipation of angular momentum before the formation of a planetary system of finite bodies. The difficulty of this point can be seen from the fact that even in our own planetary system there is no consensus concerning the amount of mass in the solar nebula in the beginning, as som einvestigators advocate a value of $m/M=0.1$ while others use considerably smaller values.

Since the actual size of any planetary system must be equal to or less than the upper limit, we have for our own planetary system $a_1 \geq a_s$. It then follows from equations (17) and (18) that

$$\frac{m}{M_\odot} \leq \frac{\Omega_o}{a_s V_s M_\odot} + \left(\frac{R_\odot}{a_s}\frac{v_m}{V_s}k^2\right)x_1 \qquad (26)$$

The ratio $m/M$ for the solar system at present is equal to $1.3\times10^{-3}$. In the early days it must be much greater than this value. If we now take $v_m$ to be the same as that determined in Table 1 (200 Km/sec), we have

$$\frac{R_\odot}{a_s}\frac{v_m}{V_s}k^2 = 5.9\times10^{-4} \qquad (27)$$

Therefore, it follows from equation (26) that if $\Omega_0=0$, $x_1>2.2$. Equation (1) shows that the probability of having $x>2.2$ is rather small. This would put our planetary system as an unusual case, namely its chance of occurrence is small. The other alternative is that $\Omega_0$ is appreciable. This means that a significant portion of the angular momentum that is now found in our planetary system has never belonged to the sun. The present consideration cannot decide which alternative is the more plausible one.

Thus, we have seen many uncertainties concerning planetary systems around the stars in general. They cannot be resolved for the time being. What we can predict from the present simple theory is that the size of a planetary system increases with a decrease of its total mass and that the distribution of sizes (measured by $\xi$ of the equivalent planet's orbit) behaves like a Maxwellian distribution of velocity magnitudes at the lower end and is truncated at the upper end. For O, B and A stars the truncation occurs at relatively small values. Therefore unless $\Omega_0$ has a large variation among individual systems, their sizes do not vary greatly from one to the other. Most of them are crowded at the upper limit. The truncation of systems around F-type stars occurs at relatively larger values. Consequently, the spread of sizes is also larger, although there is still an appreciable number of them at the upper limit of their size. On the other hand, the sizes of planetary systems around late-type (later than F) stars are expected to be distributed like a complete Maxwellian curve with a wide spread of values. They should not show the tendency to accumulate at any particular size like systems around early-type stars do. All these consequences would be modified if $\Omega_0$ varies greatly from one system to another; in such cases the distribution of planetary sizes can be derived only when we know the variation of $\Omega_0$.

Finally, we would like to ask if it is possible that there is no mass left after the actual processes of star formation (i.e., $m=0$). In that case no planet would be formed. Indeed from the point of view of star formation we do not have any compelling reason to assure us that there must be some mass left behind to form planets after the star itself is formed. On the other hand, the rotational behavior of stars does suggest that there must be some mass left behind since axial rotation could not be effectively braked without the presence of such mass around the star, although we cannot at present estimate the amount of mass that is there. It is therefore the main point of this paper, if nothing else, to show the behavior of axial rotation of stars indicates the high probability of occurrence of planetary systems around stars.

The present paper perhaps represents the first serious attempt to link the problem of occurrence of planetary systems in the stellar universe with some observational facts. The uncertainties in both theory and observation force us to adapt an over-simplified model. Thus, it should be regarded as a pioneer exploration of a nebulous field of learning rather than a legitimate treatment of something that is clearly understood. As a result we emphasize only the qualitative conclusions that have been derived here.

It is my pleasure to express my thanks to Mr. Clarence Wade, Jr. for the numerical integrals in equations (7) and (8) on the IBM 7094 digital computer at Goddard.

## REFERENCES


ALLEN, C. W., 1955, Astrophysical Quantities (London: Athlone Press).

CHANDRASEKHAR, S. and MÜNCH, G. 1950, Ap. J., **111**, 142.

EDGEWORTH, K. E., 1946, M.N. **106**, 470, 476 and 484.

FOWLER, W. A., GREENSTEIN, J. L. and HOYLE, F., 1962, Geophys. J. R.A.S. **6**, 148.

HAYASHI, C., 1961, Pub. Astr. Soc. Japan, **13**, 450.

HOYLE, F., 1960, Quarterly J.R.A.S. **1**, 28.

HUANG, S. -S., 1953, Ap. J., **118**, 285.

HUANG, S. -S., 1959, P.A.S.P. **71**, 421.

HUANG, S. -S., and STRUVE, O., 1954, Ann. d'Ap. **17**, 85.

HUANG, S. -S. and STRUVE, O., 1960, "Stellar Atmospheres" Ed. J. L. Greenstein (Chicago, Chicago University Press) Chap. 8. p. 321.

KUIPER, G. P., 1935, P.A.S.P. **47**, 15 and 121.

POVEDA, A., 1954, Nature **202**, 1319.

SCHATZMAN, E., 1962, Ann. d'Ap. **25**, 18.

SLETTEBAK, A., 1949, Ap. J. **110**, 498.

STRUVE, O., 1930, Ap. J. **72**, 1.

STRUVE, O., 1945, Pop. Astr. **53**, 201 and 259.

# SEQUENCE OF EVENTS IN THE EARLY PHASE OF THE SOLAR SYSTEM*

SU-SHU HUANG†

The purpose of this note is to construct a sequence of events in the early phase of the solar system by bringing together several recent theories in different fields of learning. First we show that these theories are mutually salutary. Thus, when we put them together, a reasonably clear picture of the formation of the planetary system emerges.

In a recent investigation by Fowler, Greenstein and Hoyle (1) (2), it has been assumed that there was strong magnetic activities on the surface of the primeval sun. The light elements, lithium, beryllium and boron were then produced according to them by spallation processes when high-energy particles (mainly protons), which had been accelerated by the electromagnetic force on the solar surface, bombarded the dense material in the solar nebula. Furthermore, they have concluded from observed fact that at the time of being bombarded the planetesimals in the solar nebula must be on the average of 12 meters in radius if their shape was spherical.

In the meantime Hayashi (3) (4) has shown that the premain sequence stars must be in a convective equilibrium. He and his associates have calculated evolutionary tracks in the H-R diagram for these stars of several masses including the solar mass. Their results differ from the previous model based on the radiative equilibrium (5) (6) by the high luminosities in the early phase of the evolution before the main sequence.

In a paper by Faulkner, Griffiths and Hoyle (7), a question as regards the consistency between Fowler's and Hayashi's theory has been raised, because in Fowler's theory, it is required that the temperature in the solar nebula must be low—a requirement that appears to contradict the high luminosity obtained by Hayashi. However, in a recent article (8) we have argued that the temperature in the solar nebula can be low even when the luminosity of the primeval sun is high if the solar nebula is opaque enough in the directions in the plane of disk (9) (10). Since the charged particles which follow the magnetic lines do not necessarily travel in the plane of disk, the high density in the disk does not prevent charged particles to bombard the planetesimals in the disk.

More recently, Poveda (11) has presented a theory of flare stars. The success of his theory for explaining the location of these stars in the H-R diagram indicates the sound reasoning of his arguments. Now, if we follow the same reasoning as he does in his investigation of flare stars, we can immediately conclude that not only Hayashi's theory presents no difficulty to Fowler's theory, but the two are mutually conducive. In order to see this point, we have to describe briefly Poveda's theory.

The flare stars show very rapid and non-periodic change in brightness (12). They are always dwarfs stars of late spectral types. It has long been suggested that the flare stars obtain their variations of luminosity in a similar manner as the solar flares do (13) (14). Since it is generally known that solar flares are a result of magnetic activities which are in turn caused by convective motion and differential rotation (15), Poveda argues that flares must be very active when stars are undergoing evolution where convection dominates. From the calculated results of Hayashi and his associates (4), Poveda is able to plot a

*Published in *the Astronomical Society of the Pacific* 77:42, February 1965.

†Goddard Space Flight Center and Catholic University, Washington, D.C.

curve in the H-R diagram on which convection stops to be a dominant factor. Thus the flare stars should all lie on that side of the curve where convection dominates and none on the other side. Indeed, that is just what has been observed.

Then we have Schatzman's theory (16) of braking axial rotation of stars due to magnetic activities. Schatzman also invokes convective motion in the early phase of stars as the cause for magnetic activities and thereby explains why axial rotation of the main-sequence stars stops at about F5 (17). In the case of the solar system, it is very difficult to understand the present distribution of angular momentum with its high concentration in major planets as representing the original state. Schatzman's theory provides an effective mechanism for braking the rotation of the primeval sun.

Thus, we have seen three theories (Fowler's, Poveda's and Schatzman's) which predict results in agreement with observed facts and at the same time all consistently require intensive magnetic activities in the primeval sun and one theory (Hayashi's) which satisfactorily explains the loci of new stars in the H-R diagram and, at the same time, provides the clue why there should be intense magnetic activities. All these four theories not only predict observed phenomena but also have strong theoretical base. Hence, the appearance of magnetic activities in the primeval sun may be regarded as an established fact.

It follows that we should inquire whether there are indeed magnetic activities in *T* Tauri stars and flare stars that are now evolving toward the main sequence. It appears that no such stars are on the list of magnetic stars discovered by Babcock (18). However, it should be noted that the magnetic field of a star has a good chance to be discovered only when it is systematic like that of a dipole field. When the magnetic activities in stars are chaotic as are envisaged by the previous theories, the lines of force are oriented at random. Hence, they are difficult to be discovered by polarization measurements.

Hayashi and his associates (4) have given the time at which the primeval sun stopped to be completely convective to be less than $10^6$ years from the time of its initial condensation and the time at which the "hydrogen burning" began to be about $25\times10^6$ years. If we follow Poveda that the solar surface activities of the primeval sun became reduced to the present level when the evolutionary track based on the convective model meets that of the radiative model, the time of intensive magnetic activities proposed by Fowler and others would be confined to the first $8\times10^6$ years of the formation of the system. This is the time that has generally been accepted as the gravitationally contracting time of the sun (1). If the intensive magnetic activities occurred only when the sun was completely convective, the formation of planetesimals of an average radius of 12 meters must have taken place in the first $10^6$ years after the sun attended hydrostatic equilibrium. It is conceivable that the magnetic activities were more intense at the very early stage when the luminosity was high and convection complete than at later stages. If so, we may indeed expect that the formation of the planetesimals occurred in the first few $10^6$ years.

Another supporting fact for the shorter time scale for the formation of planetesimals comes from a recent study by Hunger (19), who claims that contrary to the previous understanding (20) (21), T Tauri stars do not rotate rapidly because he has found many sharp stellar lines in three of these stars. He attributes the broad features previously believed to be due to axial rotation now to the blending of lines. It follows from his conclusion that axial rotation has already been reduced by magnetic braking before the evolving star becomes a T Tauri star.

We can now reconstruct the sequence of events in the early phase of the solar system from the previous and other theories. The early phase of evolution of the sun (or for that matter, any star) has often been divided into two stages: (1) the condensing or collapsing stage characterized by hydrodynamic inflow of matter and (2) the stellar stage characterized by hydrostatic equilibrium. According to recent studies (22) (23), the first stage is catastrophic if we neglect the effect of angular momentum and magnetic field. Gaustad (23) gives a time scale of $5\times10^5$ years for complete free-fall from interstellar densities to stellar conditions. The presence of a net angular momentum in the cloud prolongs somewhat the time of collapse. But from a consideration of the average angular momentum of the entire solar system observed at present we find that the effect of angular momentum on the time scale is small. Hence,

we may take one half to one million years as the time that the sun underwent the first stage. The time scale of the second stage follows results given by Hayashi and his associates (4).

The early phase of evolution of the planetary system can be divided into two corresponding stages. The transition occurred when the evolution of the sun itself was at its second stage.

As masses were falling into the protosun, accumulation of mass by direct capture of non-volatile matter (24) (25) (26) to form small local condensations far away from the primeval sun took place in what may be regarded as the primeval solar nebula which was then distributed in a spherical symmetry with respect to the sun. We may regard it as the outermost layers of infalling material at low temperatures.

According to a recent investigation by Donn and Sears (27), the particles first formed in the solar nebula are expected to be filaments and thin platelets which they call whiskers. When the whiskers are collected together they form loosely compacted instead of solidly packed condensations. Thus, the condensations in the solar nebula would have a structure resembling the lint-balls under beds or balls made of tumbleweeds that roll in the wind over the prairie under the fall sky.

Regarding the mass of these local condensations we may take the clue from Fowler's planetesimals which may be estimated from their radii to be $10^{10}$ gm on the average. For various reasons, a density of $10^{-9}$ gm/cm$^3$ has often been assumed for the flattened solar nebula. With this density the rate of growth of condensations by direct accumulation of mass can be calculated (24) (25). It grows about 1 cm in radius in ⅓ to 30 years, independent of the size of the body itself (25). In the spherical distribution before flattening, the density must be less than $10^{-9}$ (say $10^{-11}$ to $10^{-13}$) and the rate of growth would be correspondingly slower. However, it may be noted that the previous rate was obtained (25) by assuming that the accumulating body is solidly packed. For the porus body the rate of growth in radius is faster by a factor inversely proportional to the ratio of the over-all density to the mass density of the porus body. Thus, we estimate the time of formation of condensations of mass comparable to Fowler's planetesimals to be about $10^6$ years. The formation took place when the solar nebula was spherical distributed. This time scale is consistent with the time scale of solar evolution. It also agrees with the fact that the orbits of comets now observed are randomly oriented, indicating that the local condensations took place when the solar nebula was still spherical.

When strong magnetic activities appeared in the sun in its second stage of evolution before reaching the main sequence, the transfer of angular momentum from the sun to the solar nebula induced inevitably the collapse of the solar nebula from a spherical distribution to a disk one. This marks the transition of the evolution of the solar nebula from the first to the second stage. Therefore, the transition from the first stage to the second stage for the sun and that for the solar nebula are not supposed to occur at the same time but differ by an interval which covers the time for developing strong magnetic fields in the sun from hydrodynamic motion and for transporting angular momentum outward.

The local condensations might be temporarily heated up and perhaps melt during the collapse, or a rapid accumulation of matter in the process might fill their porus matrix. In any case the local condensations must have lost their porus nature and became planetesimals that Fowler envisaged when they were settled down in the rotating disk to be bombarded by high-energy particles from the sun. The collapse of the solar nebula from a spherical to a disk distribution being about 100 years if the nebula extended not far beyond Pluto's orbit, we may regard that these planetesimals received all their dosage of bombardment when they were already in the rotating disk.

The solar nebula has a life time of $2\times10^8$ years (25). Therefore, the formation of planets from the planetesimals must have taken place in a time scale less than this value. By considering first direct capture and then gravitational accretion, Kuiper (25) has found that this time scale is only barely enough to form planets. However, we are inclined to suggest that the formation of planets from planetesimals may take a much shorter time than this. Our reasoning rests on the fact that the planetesimals are gravitationally unstable. One can easily visualize this instability by imagining a large number of planetesimals floating in

space. A slight increase in density at one point (due to statistical fluctuations) will easily cause a rapid inflow of these bodies to that point, thereby producing a condensation of the planet size. If so, the time of formation is simply the free-falling time. Since the free falling started from a density of $10^{-9}$ which is more than $10^{10}$ times the interstellar density, the free-falling condensation of proto-planets would take only a few years.

Two points should be noted here however. First, this kind of gravitational instability is not what is known as Jeans instability which applies to a gaseous medium (28). Secondly, the present instability would be damped when gas and dust are present together with planetesimals. Therefore, it might take a longer time to form major planets. In any case, it is very likely that when the sun reached the main sequence stage (i.e., when energy dissipated is completely balanced by energy produced by thermonuclear reactions of converting hydrogen into helium), the solar system was practically in the same state as it is now found.

We now propose that because of the difficulty of transporting angular momentum to great distances, the collapse of the solar nebula into a disk occurred only in the solar neighborhood, perhaps not far beyond the orbit of Pluto. Local condensations within this limit must all have fallen into the disk. For even if they survived the initial collapse, their later crossings of the disk, which reduce their vertical velocity component, would force them to follow the general motion of gas and dust in the disk.

The local condensations contained in that part of the spherical distribution that did not undergo the collapse continued their accretion of matter by direct capture until the remnant of the solar nebula was completely dissipated. We have mentioned that at the time of formation of the disk, the local condensations had an average mass of about $10^{10}$ gm each. Further accretions made these condensations to reach the comet masses of $10^{15}-10^{17}$ gm each. Since these condensations have not suffered catastrophic collapse and have remained far away from the sun all the time, they maintain the porous nature till today as comet nuclei (29).

It follows from the above considerations that comets must have been much more numerous in the early days of the solar system, because there was a large volume (corresponding to the uncollapsed portion of the solar nebula) which contained these cometary nuclei. Gradually, however, the cometary nuclei were perturbed by planets either to the vicinity of the sun and were then disintegrated or to large distances from the sun and were thereby survived. The latter forms the reservoir of comets at large distances from the sun from which the present observable comets come as a result of stellar perturbation. Except by putting the original formation beyond the orbit of Jupiter, the present picture follows what has been proposed by Oort (30).

We have seen that events in the early phase of the solar system formed a natural sequence one necessarily leading to the next. Consequently, we have now good reasons to expect that the existence of planetary systems around main-sequence stars, especially of spectral type later than F5 where axial rotation stops, must be common in the universe as has been heuristically suggested before (31).

It is a pleasure to acknowledge my sincere thanks to Dr. A. Poveda for letting me read his paper before publication. It is his paper that induced me to prepare this note.

## REFERENCES

1. W. A. Fowler, Science, **135**, 1037 (1962).
2. W. A. Fowler, J. L. Greenstein and F. Hoyle, Geophys. J.R.A.S., **6**, 148 (1962).
3. C. Hayashi, publ. Astr. Soc. Japan, **13**, 450 (1961).
4. C. Hayashi, R. Hoshi and D. Sigimoto, Progress. Theor. Phys. Suppl. No. 22 (1962).
5. R. D. Levée, Astrop. J. 117, 200 (1953).
6. L. G. Henyey, R. LeLevier and R. D. Levée, publ. Astr. Soc. Pacific, **67, 154** (1955).
7. F. Faulkner, K. Griffiths and F. Hoyle, Mon. Notices R.A.S. **126,** 1 (1963).
8. S. -S. Huang, Sky and Telescope, **28,** 13 (1964).
9. B. Y. Levin, "The Origin of the Earth and the Planets" (Foreign Languages publ. House, Moscow ed. 2, 1958).
10. E. J. Öpik, Icarus **1, 200** (1962).
11. A. Poveda, pre-publ. print (1964).
12. G. Haro, "Non-stable stars" (Cambridge University Press, Cambridge, 1957) p. 26; "Symposium of Stellar Evolution" (Astr. Obs. La Plata, 1962).
13. G. R. Burbidge and E. M. Burbidge, Observatory, **75, 212** (1955).
14. L. Bierman and R. Lüst, "Stellar Atmospheres" (University of Chicago Press, Chicago, 1960) p. 260.

15. E. Parker, Astrop. J. **121**, 491; **122**, 293 (1955).
16. E. Schatzman, Ann. d'Astrop., **25**, 18 (1962).
17. O. Struve, Astrop. J., **72**, 1 (1930).
18. H. W. Babcock, Astrop. J. Suppl., **3**, 141 (1953).
19. K. Hunger, Zeits. f. Astrop. **56**, 285 (1963).
20. G. H. Herbig, J. Roy. Astr. Soc. Canada, **46**, 222 (1952); Astrop. J. **125**, 612 (1957); "Symposium on Stellar Evolution" (Astr. Obs. La Plata, 1962) p. 23.
21. S. -S. Huang and O. Struve, "Stellar Atmospheres" (University of Chicago Press, Chicago, 1960) p. 321.
22. A. G. W. Cameron, Icarus, **1**, 13 (1962).
23. J. E. Gaustad, Astrop. J., **138**, 1050 (1963).
24. S. Chandrasekhar, Rev. Mod. Phys., **18**, 94 (1946).
25. G. P. Kuiper, "Astrophysics" (McGraw-Hill Book Co., New York, 1951) p. 357.
26. H. E. Urey, "The Planets" (Yale University Press, New Haven, Conn. 1952).
27. B. Donn and G. W. Sears, Science, **140**, 1208 (1963).
28. J. H. Jeans, "Astronomy & Cosmogony" (Cambridge University Press, Cambridge 1928).
29. F. L. Whipple, Astrop. J., **111**, 375 (1950).
30. J. H. Oort, Bull. Astr. Netherlands **11**, 91 (1950).
31. S. -S. Huang, publ. Astr. Soc. Pacific **71**, 421 (1959).

# PLASMA NEUTRINO EMISSION FROM A HOT, DENSE ELECTRON GAS*

CULLEN L. INMAN† AND MALVIN A. RUDERMAN‡

Neutrino pair emission from coherent electrone excitations (transverse plasmons) in a hot, dense stellar plasma is calculated for a regime of temperatures and densities relevant to stellar evolution. Detailed numerical results are presented for temperatures in the range $4\times10^7$–$5\times10^8$ °K and densities in the range $10^4$–$10^8$ gm/cm³.

## I. INTRODUCTION

A coupling of electron and neutrino pairs is implied by almost all models which describe the weak Fermi interactions of elementary particles. Although there has not yet been any direct experimental detection of such an electron-neutrino coupling, it is a necessary consequence of the apparent existence (Brookhaven 1963) of an intermediate heavy charged boson in $\beta$-decay. Moreover the form and magnitude of the resulting electron-neutrino interaction are unambiguously determined. The strength of the coupling is characterized by the small Fermi constant

$$g\sim3.08\sim10^{-12}\frac{\hbar^3}{m_e{}^2c},$$

where $m_e$ is the electron mass; its form is analogous to the interaction of electromagnetic radiation with the electron current. An accelerated electron can then radiate a neutrino ($\nu$)–antineutrino ($\bar{\nu}$) pair with the same matrix element as that for electromagnetic radiation but with greatly reduced probability. For example in an atomic transition of energy $E$ the probability $R_{\nu\bar{\nu}}$ for radiation of $\nu\bar{\nu}$, relative to $R_\gamma$, that for radiating a photon, is only

$$\frac{R_{\nu\bar{\nu}}}{R_\gamma}\sim\frac{g^2E^4}{e^2\hbar^5c^5}\sim10^{-21}\left(\frac{E}{m_ec^2}\right)^4. \tag{1}$$

The probability for emitting a $\nu\nu$ pair rises rapidly with energy (in this case, like $E^7$) but even an electron-positron pair will annihilate into $\nu\nu$ rather than a pair of gamma rays only about once in $10^{22}$ times.

An extremely strong energy dependence is characteristic of all mechanisms for radiating $\nu\nu$ pairs: an electron moving with frequency $\omega$ in a classical circular orbit of radius $R$ radiates electromagnetic waves, gravitational waves, and neutrino pairs with powers, $P$, that follow from simple dimensional considerations:

$$P_\gamma\sim\frac{e^2}{c^3}R^2\omega^4, \tag{2}$$

$$P_{\text{Grav}}\sim\frac{Gm_e{}^2R^4\omega^6}{c^5}\quad\text{(quadrupole)}, \tag{3}$$

and

$$P_{\nu\nu}\sim\frac{g^2R^2\omega^8}{hc^8}. \tag{4}$$

At low frequencies neutrino pair processes are entirely negligible. For a double star in which each member has a different electron molecular weight, the center of electron charge rotates about the fixed center of mass, but the neutrino pair radiation is smaller by perhaps eighty orders of

*Published in *The Astrophysical Journal*, 140(3): 1025–1040, October 1, 1964. This work was supported in part by the National Science Foundation.

†Goddard Space Flight Center and New York University.

‡New York University, on leave from the University of California, Berkeley, California.

magnitude than the small quadrupole radiation of gravitational waves. High frequencies ($\omega \gtrsim 10^{18}$ ~1 keV), sufficient for significant $\nu\nu$ radiation by electrons, are available only on the microscopic scale where electrons are strongly accelerated by photons or intimate collisions.

Mechanisms for the radiation of $\nu\nu$ pairs by electrons within a star include the following:

(a) $\gamma+e\rightarrow e+\nu+\nu$, (photoneutrinos) (Ritus 1962; Ida and Vahara; Chiu and Stabler 1961)

(b) $e^-+e^+\rightarrow\nu+\nu$, (pair annihilation neutrinos) (Chiu and Morrison 1960; Chiu 1961)

(c) $e$+Coulomb field$\rightarrow e+\nu+\nu$, (neutrino bremsstrahlung) (Gandel'man and Pineau 1960)

(d) $\gamma$+Coulomb field$\rightarrow\nu+\nu$, (photonuclear neutrinos) (Rosenberg 1963; Matinyan and Tsilosani 1962)

(e) $\gamma+\gamma\rightarrow\gamma+\nu+\nu$, (van Hieu and Shabalin 1963)

(f) plasma excitation$\rightarrow\nu+\nu$. (plasma neutrinos) (Adams, Ruderman, and Woo 1963).

Processes (a), (b), and (f) are the dominant ones in those regimes of density and temperature typical of stellar interiors (Reeves 1963). Photo and pair annihilation neutrino emissions have exact analogues in Compton scattering and the two-photon annihilation of an electron-positron pair. The main contribution to process (d) arises from the electron current associated with a transverse ($E$ perpendicular to $k$) electromagnetic wave moving through the plasma.

## II. PLASMA NEUTRINOS

Plasma neutrino emission has been calculated by Adams, Ruderman, and Woo (1963) for any medium whose dielectric constants are known functions of frequency and wave-number. The relevant dielectric constants have also been evaluated for an electron gas which may be relativistic and degenerate. For a plasma frequency $\omega_o$ such that $(\hbar\omega_o)^2 \ll 4(m_e c^2)^2$ the relevant transverse dielectric constant is well approximated by

$$\epsilon^t = 1-\frac{\omega_o^2}{\omega^2}, \tag{5}$$

with

$$\omega_o^2=\frac{4\pi e^2}{m_e}\int dp f(p)\left(1-\frac{p^2c^2}{3E_p^2}\right)\frac{m_e c^2}{E_p}. \tag{6}$$

Here $f(p)$ is the momentum distribution function for the electrons and

$$E_p=(p^2c^2+m_e^2c^4)^{1/2}. \tag{7}$$

The dielectric constant of equation (5) leads to a greatly simplified neutrino pair emissivity $Q_t$(erg/sec/cm$^3$):

$$Q_t=\frac{g^2\omega_o^6}{12\pi^4c^2\hbar^5}\int_0^\infty k^2dk(e^{\omega\beta}-1)^{-1}, \tag{8}$$

with $\omega=(\omega_o^2+k^2c^2)^{1/2}$ and $\beta=(k_BT)^{-1}$. The function $Q_t$ computed from equations (6) and (8) is given as a function of density and temperature in Section III.

The form of equation (8) can be inferred in a rather straightforward way from equation (5). For a transverse electromagnetic wave in a plasma with the dielectric constant the dispersion relation is

$$\omega^2=k^2c^2+(1-\epsilon)\omega^2=k^2c^2+\omega_o^2. \tag{9}$$

Therefore such waves, when quantized, behave as if they were relativistic particles of mass $\hbar\omega_o/c^2$, and they are energetically unstable against the decay into a neutrino pair. If $r$ is the decay rate for such a particle at rest, its decay rate when moving is decreased by the usual relativistic time dilatation to $(r\omega_o/\omega)$ and its rate of production of $\nu\nu$ becomes $(r\omega_o/\omega)\hbar\omega=r\hbar\omega_o$. Thus the total neutrino emissivity per unit volume is

$$Q_t\sim r\hbar\omega_o 8\pi\int\frac{k^2dk}{(2\pi)^3}(e^{\beta\omega}-1)^{-1}. \tag{10}$$

The integral is just the total number of "photons" of mass per unit volume in a canonical Einstein-Bose distribution. We need only calculate the $\nu\nu$ emission $r\hbar\omega_o$ caused by the oscillating electric field with $\omega=\omega_o$ and infinite wavelength ($k=0$). When $k=0$ this mode is identical to the usual plasma oscillation; the accelerated electrons oscillating in phase with frequency $\omega_o$, amplitude $x$, and acceleration $\omega_o^2x$ coherently radiate neutrino pairs. But because of the finite neutrino wavelength $\lambda_\nu\sim c/\omega_o$ all of the electrons in a large volume $\Omega$ can not radiate as if they constituted a

single highly charged particle. Rather only those electrons in a cube of volume $\sim(\lambda_\nu)^3$ effectively radiate coherently. Then from a large volume $\Omega$ with electron density $n$, the total rate of neutrino energy emission $P$ can be estimated from equation (4):

$$P\sim\frac{g^2\omega_o{}^8x^2}{hc^8}(n\lambda_\mu{}^3)^2\frac{\Omega}{(\lambda_\nu)^3}, \tag{11}$$

with

$$\lambda_\nu=\frac{c}{\omega_o}. \tag{12}$$

The additional kinetic energy of the oscillating electrons is $\frac{1}{2}m\omega_o{}^2x^2n\Omega$. This energy together with an equivalent average potential energy must total $h\omega_o$ when the oscillation amplitude is quantized to correspond to a single quantum of excitation (plasmon). Thus

$$m\omega_o{}^2x^2n\Omega=h\omega_o. \tag{13}$$

The combination of equations (11), (12), and (13) yields $P$ for a single plasmon at rest, i.e., $rh\omega_o$:

$$h\omega_o r\sim\frac{g^2}{c^5}\omega_o{}^4\frac{n}{m}. \tag{14}$$

But

$$\omega_o{}^2\sim4\pi ne^2/m, \tag{15}$$

so that

$$h\omega_o r\sim\frac{g^2}{c^2}\frac{\omega_o{}^6}{c^5}. \tag{16}$$

Equations (16) and (10) yield equation (8).

## III. EXACT CALCULATION OF THE TRANSVERSE EMISSIVITY

### (a) Introduction

In Section II it was shown that the rate of loss of energy in neutrino pairs due to decay of transverse plasmons is

$$Q_t=2g^2(3\pi e^2)^{-1}(2\pi)^{-3}\omega_o{}^6\sum_1^\infty\int^\infty \exp(-n\beta\omega)k^2dk. \tag{17}$$

The units are $h=m_e=c=1$. Here $g=3.08\times10^{-12}$ is the weak coupling constant; $\omega$ is given by the dispersion relation for the transverse plasmons, $\omega^2=\omega_o{}^2+k^2$; and

$$\omega_o{}^2=4e^2p_F{}^3/3\pi E_F) \tag{18}$$

is the plasma frequency. Of course $\beta=1/k_BT$). We take $\mu_e=2$.

We define a function $\mathfrak{F}(x)$ of $x$ alone by

$$\mathfrak{F}(x)=\sum_1^\infty\int_0^\infty \exp[-nx\cosh\xi]\sinh^2\xi\cosh\xi d\xi. \tag{19}$$

By considering the dispersion relation and equation (17) one sees that

$$Q_t=2g^2(3\pi e^2)^{-1}(2\pi)^{-3}\omega_o{}^9\mathfrak{F}(\beta\omega_o), \tag{20}$$

and we may note that the expression for the number density of a gas of bosons at zero chemical potential is

$$\frac{N}{V}=\frac{1}{\pi^2}\left(\frac{mc}{\hbar}\right)^3\mathfrak{F}(\beta mc^2). \tag{21}$$

Apart from care in handling the conversion of units we need then only discuss the calculation of $\mathfrak{F}(x)$.

### (b) The Function $\mathfrak{F}$ (x)

1. *Small ($x\leq0.5$) values of the argument.*—It is shown in the Appendix that for $x<2\pi$ there exists an expansion of $x^3\mathfrak{F}(x)$; note

$$\zeta(3)=\sum_{n=1}^\infty(1/n^3).$$

Truncating it,

$$\mathfrak{F}(x)\doteq\frac{1}{x^3}\left[\left[2\zeta(3)+\frac{1}{2}x^2\ln x-\frac{1}{4}(2\ln2+1)x^2+\frac{1}{96}x^4\ln x-\frac{1}{96}\left\{\ln2-\frac{1}{4}+\ln2\pi+\left[-\frac{\zeta'(2)}{\zeta(2)}\right]\right\}x^4\right]\right]. \tag{22}$$

For $x=0.5$ this gives a result which differs from that obtained by summing the Hankel series (see subsection 2 below) by one part in $10^6$. It will also be seen that by taking only the constant term in the square brackets, and using equation (20), we get just the equation preceding equation (28) in Adams *et al.* (1963).

2. *Intermediate and large values of the argument ($x\geq0.5$).*—Chandrasekhar (1957) gives a result (p. 398, eq.[252] and [248] that, omitting the

minus signs and $\Lambda$, since we have bosons at zero chemical potential, reads

$$\mathfrak{F}(x)=\sum_{n=1}^{\infty}\frac{K_2(nx)}{nx}\doteq\sum_{n=1}^{M}\frac{K_2(nx)}{nx}, \qquad (23)$$

where $K_2(z)$ is the modified Bessel function of the second kind, of order 2. The criterion for the choice of $M$ is discussed in subsection 3. The series equation (23) is a Hankel series, similar to a Dirichlet series, and converges for all $x$, albeit very slowly for small $x$: (see Greenwood [1941]). Note that for small $\xi$, $K_2(\xi)\approx 2/\xi^3$, so that substituting this expression in equation (23) we get again

$$\mathfrak{F}(x)\approx\frac{2}{x^3}\sum_{n=1}^{\infty}\left(\frac{1}{n^3}\right)=\frac{2\zeta(3)}{x^3},$$

for small $x$, just what one obtains by taking only the *zero*th-order term in braces in equation (22).

For large $\xi$, on the other hand, $K_2(\xi)\approx(\pi/2\xi)^{1/2}e^{-\xi}$, and if we take only the first term of equation (23), using this expression as an approximation for it, we get $\mathfrak{F}(x)\approx(\pi/2)^{1/2}x^{-3/2}e^{-x}$, for large $x$.

If one uses this last plus equation (20) one gets just the equation preceding equation (29) in Adams *et al.* (1963).

3. *Error terms.*—For equation (22), the small argument form, it is shown in the Appendix that the lowest order neglected term is $O(x^6\ln x)$. The coefficient multiplying this term will be quite small.

For equation (23), the intermediate and large form, we break off the sum when

$$\frac{K_2(Mx)}{Mx}<10^{-6}\frac{K_2(x)}{x}.$$

By approximating, for large $M$, the remainder term by

$$\sum_{n=M+1}^{\infty}\frac{K_2(nx)}{nx}\approx\frac{1}{x}\int_{M+1/2}^{\infty}\frac{K_2(nx)}{n}dn$$

$$=\frac{1}{x}\frac{K_1[(M+\tfrac{1}{2})x]}{(M+\tfrac{1}{2})x}<\frac{1}{x}\frac{K_2(Mx)}{Mx},$$

we find that the error is less than $(1/x)\times10^{-6}$ times the first term. This is for the range 0.5–5, since for larger values we have no need of many terms.

### (c) Conversion of Units

The dimensions of $Q_t$ are erg/cm$^3$/sec. In the units in which equation (20) is given, units of energy, length, and time are $m_ec^2$, $\hbar/m_ec$, and $\hbar/m_ec^2$, respectively. Thus $Q_t$ in c.g.s. units is

$$Q_t=\frac{m_ec^2}{(\hbar/m_ec)^3}\frac{1}{\hbar/(m_ec^2)}\left[\frac{2}{3\pi}\times137.04\times(3.08\times10^{-12})^2\frac{1}{(2\pi)^3}\right]+\left(\frac{\hbar\omega_o}{m_ec^2}\right)^9\mathfrak{F}(\beta\hbar\omega_o)=$$

$$=1.228\times10^{22}\left(\frac{\hbar\omega_o}{m_ec^2}\right)^9\mathfrak{F}(\beta\hbar\omega_o), \qquad (24)$$

where now all dimensioned quantities are in c.g.s. units. In c.g.s. units

$$p_F{}^3=3\pi^2N_{\mathrm{AVO}}\frac{1}{\mu_e}\rho=\frac{3}{2}\pi^2N_{\mathrm{AVO}}\,\rho.$$

Thus in c.g.s. units

$$\hbar^2\omega_o{}^2=2\pi(\hbar c)^2\left[1+\left(\frac{\hbar}{m_ec}\right)^2\left(\frac{3}{2}\pi^2N_{\mathrm{AVO}}\,\rho\right)^{2/3}\right]^{-1/2}N_{\mathrm{AVO}}\frac{e^2}{m_ec^2}\rho$$

or

$$\hbar\omega_o=3.265\times10^{-11}(1+6.413\times10^{-5}\rho^{2/3})^{-1/4}\rho^{1/2}, \qquad (25)$$

where now all dimensioned quantities are in c.g.s. units.

In c.g.s. units

$$\beta=\frac{7.244\times10^8}{T_7}, \qquad (26)$$

where $T_7$ is the temperature in units of $10^7$ °K.

Using equations (25) and (26) in equation (24) we can compute $Q_t$ for given values of $\rho$ and $T$. Of course

$$q_t=\frac{Q_t}{\rho}.$$

Table 1 gives $q_t$ as a function of $\rho$ and $T$.

TABLE 1.—*Neutrino Emissivity by Transverse Plasmons*

| $T$ | $q$ sub $T$ | $T$ | $q$ sub $T$ | $T$ | $q$ sub $T$ |
|---|---|---|---|---|---|
| log rho = 4.00 | | | | | |
| $.40000\times10^{8}$ | $.30491\times10^{-2}$ | $.20000\times10^{9}$ | $.43162\times10^{0}$ | $.36000\times10^{9}$ | $.25327\times10^{1}$ |
| $.60000\times10^{8}$ | $.10963\times10^{-1}$ | $.22000\times10^{9}$ | $.57531\times10^{0}$ | $.38000\times10^{9}$ | $.29796\times10^{1}$ |
| $.80000\times10^{8}$ | $.26678\times10^{-1}$ | $.24000\times10^{9}$ | $.74776\times10^{0}$ | $.40000\times10^{9}$ | $.34762\times10^{1}$ |
| $.10000\times10^{9}$ | $.52820\times10^{-1}$ | $.26000\times10^{9}$ | $.95157\times10^{0}$ | $.42000\times10^{9}$ | $.40251\times10^{1}$ |
| $.12000\times10^{9}$ | $.92010\times10^{-1}$ | $.28000\times10^{9}$ | $.11894\times10^{1}$ | $.44000\times10^{9}$ | $.46289\times10^{1}$ |
| $.14000\times10^{9}$ | $.14687\times10^{0}$ | $.30000\times10^{9}$ | $.14638\times10^{1}$ | $.46000\times10^{9}$ | $.52902\times10^{1}$ |
| $.16000\times10^{9}$ | $.22001\times10^{0}$ | $.32000\times10^{9}$ | $.17774\times10^{1}$ | $.48000\times10^{9}$ | $.60116\times10^{1}$ |
| $.18000\times10^{9}$ | $.31405\times10^{0}$ | $.34000\times10^{9}$ | $.21328\times10^{1}$ | $.50000\times10^{9}$ | $.67958\times10^{1}$ |
| log rho = 4.20 | | | | | |
| $.40000\times10^{8}$ | $.71282\times10^{-2}$ | $.20000\times10^{9}$ | $.10627\times10^{1}$ | $.36000\times10^{9}$ | $.62533\times10^{1}$ |
| $.60000\times10^{8}$ | $.26293\times10^{-1}$ | $.22000\times10^{9}$ | $.14174\times10^{1}$ | $.38000\times10^{9}$ | $.73579\times10^{1}$ |
| $.80000\times10^{8}$ | $.64689\times10^{-1}$ | $.24000\times10^{9}$ | $.18432\times10^{1}$ | $.40000\times10^{9}$ | $.85854\times10^{1}$ |
| $.10000\times10^{9}$ | $.12883\times10^{0}$ | $.26000\times10^{9}$ | $.23466\times10^{1}$ | $.42000\times10^{9}$ | $.99421\times10^{1}$ |
| $.12000\times10^{9}$ | $.22520\times10^{0}$ | $.28000\times10^{9}$ | $.29340\times10^{1}$ | $.44000\times10^{9}$ | $.11435\times10^{2}$ |
| $.14000\times10^{9}$ | $.34029\times10^{0}$ | $.30000\times10^{9}$ | $.36119\times10^{1}$ | $.46000\times10^{9}$ | $.13069\times10^{2}$ |
| $.16000\times10^{9}$ | $.54058\times10^{0}$ | $.32000\times10^{9}$ | $.43868\times10^{1}$ | $.48000\times10^{9}$ | $.14853\times10^{2}$ |
| $.18000\times10^{9}$ | $.77254\times10^{0}$ | $.34000\times10^{9}$ | $.52651\times10^{1}$ | $.50000\times10^{9}$ | $.16792\times10^{2}$ |
| log rho = 4.40 | | | | | |
| $.40000\times10^{8}$ | $.16221\times10^{-1}$ | $.20000\times10^{9}$ | $.25971\times10^{1}$ | $.36000\times10^{9}$ | $.15346\times10^{2}$ |
| $.60000\times10^{8}$ | $.61954\times10^{-1}$ | $.22000\times10^{9}$ | $.34674\times10^{1}$ | $.38000\times10^{9}$ | $.18061\times10^{2}$ |
| $.80000\times10^{8}$ | $.15476\times10^{0}$ | $.24000\times10^{9}$ | $.45125\times10^{1}$ | $.40000\times10^{9}$ | $.21077\times10^{2}$ |
| $.10000\times10^{9}$ | $.31071\times10^{0}$ | $.26000\times10^{9}$ | $.57483\times10^{1}$ | $.42000\times10^{9}$ | $.24412\times10^{2}$ |
| $.12000\times10^{9}$ | $.54582\times10^{0}$ | $.28000\times10^{9}$ | $.71908\times10^{1}$ | $.44000\times10^{9}$ | $.28081\times10^{2}$ |
| $.14000\times10^{9}$ | $.87607\times10^{0}$ | $.30000\times10^{9}$ | $.88559\times10^{1}$ | $.46000\times10^{9}$ | $.32100\times10^{2}$ |
| $.16000\times10^{9}$ | $.13174\times10^{1}$ | $.32000\times10^{9}$ | $.10760\times10^{1}$ | $.48000\times10^{9}$ | $.36485\times10^{2}$ |
| $.18000\times10^{9}$ | $.18858\times10^{1}$ | $.34000\times10^{9}$ | $.12918\times10^{1}$ | $.50000\times10^{9}$ | $.41251\times10^{2}$ |
| log rho = 4.60 | | | | | |
| $.40000\times10^{8}$ | $.35602\times10^{-1}$ | $.20000\times10^{9}$ | $.62850\times10^{1}$ | $.36000\times10^{9}$ | $.37354\times10^{2}$ |
| $.60000\times10^{8}$ | $.14256\times10^{0}$ | $.22000\times10^{9}$ | $.84023\times10^{1}$ | $.38000\times10^{9}$ | $.43975\times10^{2}$ |
| $.80000\times10^{8}$ | $.36355\times10^{0}$ | $.24000\times10^{9}$ | $.10946\times10^{2}$ | $.40000\times10^{9}$ | $.51335\times10^{2}$ |
| $.10000\times10^{9}$ | $.73812\times10^{0}$ | $.26000\times10^{9}$ | $.13956\times10^{2}$ | $.42000\times10^{9}$ | $.59471\times10^{2}$ |
| $.12000\times10^{9}$ | $.13055\times10^{1}$ | $.28000\times10^{9}$ | $.17471\times10^{2}$ | $.44000\times10^{9}$ | $.68424\times10^{2}$ |
| $.14000\times10^{9}$ | $.21049\times10^{1}$ | $.30000\times10^{9}$ | $.21529\times10^{2}$ | $.46000\times10^{9}$ | $.78231\times10^{2}$ |
| $.16000\times10^{9}$ | $.31753\times10^{1}$ | $.32000\times10^{9}$ | $.26170\times10^{2}$ | $.48000\times10^{9}$ | $.88931\times10^{2}$ |
| $.18000\times10^{9}$ | $.45557\times10^{1}$ | $.34000\times10^{9}$ | $.31432\times10^{2}$ | $.50000\times10^{9}$ | $.10056\times10^{3}$ |

TABLE 1.—*Neutrino Emissivity by Transverse Plasmons—Continued*

| $T$ | $q$ sub $\gamma$ | $T$ | $q$ sub $T$ | $T$ | $q$ sub $T$ |
|---|---|---|---|---|---|
| log rho = 4.80 | | | | | |
| $.40000\times10^{8}$ | $.74499\times10^{-1}$ | $.20000\times10^{9}$ | $.15011\times10^{2}$ | $.36000\times10^{9}$ | $.89949\times10^{2}$ |
| $.60000\times10^{8}$ | $.31782\times10^{0}$ | $.22000\times10^{9}$ | $.20105\times10^{2}$ | $.38000\times10^{9}$ | $.10594\times10^{3}$ |
| $.80000\times10^{8}$ | $.83355\times10^{0}$ | $.24000\times10^{9}$ | $.26232\times10^{2}$ | $.40000\times10^{9}$ | $.12372\times10^{3}$ |
| $.10000\times10^{9}$ | $.17184\times10^{1}$ | $.26000\times10^{9}$ | $.33485\times10^{2}$ | $.42000\times10^{9}$ | $.14338\times10^{3}$ |
| $.12000\times10^{9}$ | $.30679\times10^{1}$ | $.28000\times10^{9}$ | $.41959\times10^{2}$ | $.44000\times10^{9}$ | $.16501\times10^{3}$ |
| $.14000\times10^{9}$ | $.49773\times10^{1}$ | $.30000\times10^{9}$ | $.51749\times10^{2}$ | $.46000\times10^{9}$ | $.18871\times10^{3}$ |
| $.16000\times10^{9}$ | $.75411\times10^{1}$ | $.32000\times10^{9}$ | $.62947\times10^{2}$ | $.48000\times10^{9}$ | $.21457\times10^{3}$ |
| $.18000\times10^{9}$ | $.10854\times10^{2}$ | $.34000\times10^{9}$ | $.75649\times10^{2}$ | $.50000\times10^{9}$ | $.24269\times10^{3}$ |
| log rho = 5.00 | | | | | |
| $.40000\times10^{8}$ | $.14647\times10^{0}$ | $.20000\times10^{9}$ | $.35234\times10^{2}$ | $.36000\times10^{9}$ | $.21359\times10^{3}$ |
| $.60000\times10^{8}$ | $.67973\times10^{0}$ | $.22000\times10^{9}$ | $.47315\times10^{2}$ | $.38000\times10^{9}$ | $.25169\times10^{3}$ |
| $.80000\times10^{8}$ | $.18510\times10^{1}$ | $.24000\times10^{9}$ | $.61862\times10^{2}$ | $.40000\times10^{9}$ | $.29409\times10^{3}$ |
| $.10000\times10^{9}$ | $.38953\times10^{1}$ | $.26000\times10^{9}$ | $.79101\times10^{2}$ | $.42000\times10^{9}$ | $.34098\times10^{3}$ |
| $.12000\times10^{9}$ | $.70433\times10^{1}$ | $.28000\times10^{9}$ | $.99257\times10^{2}$ | $.44000\times10^{9}$ | $.39259\times10^{3}$ |
| $.14000\times10^{9}$ | $.11524\times10^{2}$ | $.30000\times10^{9}$ | $.12256\times10^{3}$ | $.46000\times10^{9}$ | $.44914\times10^{3}$ |
| $.16000\times10^{9}$ | $.17565\times10^{2}$ | $.32000\times10^{9}$ | $.14922\times10^{3}$ | $.48000\times10^{9}$ | $.51087\times10^{3}$ |
| $.18000\times10^{9}$ | $.25392\times10^{2}$ | $.34000\times10^{9}$ | $.17948\times10^{3}$ | $.50000\times10^{9}$ | $.57800\times10^{3}$ |
| log rho = 5.20 | | | | | |
| $.40000\times10^{8}$ | $.26574\times10^{0}$ | $.20000\times10^{9}$ | $.80867\times10^{2}$ | $.36000\times10^{9}$ | $.49794\times10^{3}$ |
| $.60000\times10^{8}$ | $.13778\times10^{1}$ | $.22000\times10^{9}$ | $.10898\times10^{3}$ | $.38000\times10^{9}$ | $.58734\times10^{3}$ |
| $.80000\times10^{8}$ | $.39434\times10^{1}$ | $.24000\times10^{9}$ | $.14290\times10^{3}$ | $.40000\times10^{9}$ | $.68679\times10^{3}$ |
| $.10000\times10^{9}$ | $.85295\times10^{1}$ | $.26000\times10^{9}$ | $.18314\times10^{3}$ | $.42000\times10^{9}$ | $.79683\times10^{3}$ |
| $.12000\times10^{9}$ | $.15688\times10^{2}$ | $.28000\times10^{9}$ | $.23024\times10^{3}$ | $.44000\times10^{9}$ | $.91798\times10^{3}$ |
| $.14000\times10^{9}$ | $.25962\times10^{2}$ | $.30000\times10^{9}$ | $.28475\times10^{3}$ | $.46000\times10^{9}$ | $.10508\times10^{4}$ |
| $.16000\times10^{9}$ | $.39891\times10^{2}$ | $.32000\times10^{9}$ | $.34717\times10^{3}$ | $.48000\times10^{9}$ | $.11958\times10^{4}$ |
| $.18000\times10^{9}$ | $.58015\times10^{2}$ | $.34000\times10^{9}$ | $.41806\times10^{3}$ | $.50000\times10^{9}$ | $.13534\times10^{4}$ |
| log rho = 5.40 | | | | | |
| $.40000\times10^{8}$ | $.43556\times10^{0}$ | $.20000\times10^{9}$ | $.18037\times10^{3}$ | $.36000\times10^{9}$ | $.11346\times10^{4}$ |
| $.60000\times10^{8}$ | $.26082\times10^{1}$ | $.22000\times10^{9}$ | $.24426\times10^{3}$ | $.38000\times10^{9}$ | $.13399\times10^{4}$ |
| $.80000\times10^{8}$ | $.79688\times10^{1}$ | $.24000\times10^{9}$ | $.32150\times10^{3}$ | $.40000\times10^{9}$ | $.15685\times10^{4}$ |
| $.10000\times10^{9}$ | $.17871\times10^{2}$ | $.26000\times10^{9}$ | $.41333\times10^{3}$ | $.42000\times10^{9}$ | $.18214\times10^{4}$ |
| $.12000\times10^{9}$ | $.33617\times10^{2}$ | $.28000\times10^{9}$ | $.52100\times10^{3}$ | $.44000\times10^{9}$ | $.21001\times10^{4}$ |
| $.14000\times10^{9}$ | $.56484\times10^{2}$ | $.30000\times10^{9}$ | $.64573\times10^{3}$ | $.46000\times10^{9}$ | $.24056\times10^{4}$ |
| $.16000\times10^{9}$ | $.87732\times10^{2}$ | $.32000\times10^{9}$ | $.78876\times10^{3}$ | $.48000\times10^{9}$ | $.27393\times10^{4}$ |
| $.18000\times10^{9}$ | $.12861\times10^{3}$ | $.34000\times10^{9}$ | $.95131\times10^{3}$ | $.50000\times10^{9}$ | $.31023\times10^{4}$ |

TABLE 1 —*Neutrino Emissivity by Transverse Plasmons—Continued*

| $T$ | $q$ sub $T$ | $T$ | $q$ sub $T$ | $T$ | $q$ sub $T$ |
|---|---|---|---|---|---|
| log rho = 5.60 | | | | | |
| .40000×10⁸ | .62929×10⁰ | .20000×10⁹ | .38829×10³ | .36000×10⁹ | .25132×10⁴ |
| .60000×10⁸ | .45341×10¹ | .22000×10⁹ | .52917×10³ | .38000×10⁹ | .29727×10⁴ |
| .80000×10⁸ | .15074×10² | .24000×10⁹ | .70009×10³ | .40000×10⁹ | .34846×10⁴ |
| .10000×10⁹ | .35435×10² | .26000×10⁹ | .90385×10³ | .42000×10⁹ | .40517×10⁴ |
| .12000×10⁹ | .68650×10² | .28000×10⁹ | .11433×10⁴ | .44000×10⁹ | .46767×10⁴ |
| .14000×10⁹ | .11766×10³ | .30000×10⁹ | .14211×10⁴ | .46000×10⁹ | .53624×10⁴ |
| .16000×10⁹ | .18537×10³ | .32000×10⁹ | .17402×10⁴ | .48000×10⁹ | .61116×10⁴ |
| .18000×10⁹ | .27463×10³ | .34000×10⁹ | .21033×10⁴ | .50000×10⁹ | .69271×10⁴ |
| log rho = 5.80 | | | | | |
| .40000×10⁸ | .78021×10⁰ | .20000×10⁹ | .80068×10⁰ | .36000×10⁹ | .53805×10⁴ |
| .60000×10⁸ | .71030×10¹ | .22000×10⁹ | .11003×10⁴ | .38000×10⁹ | .63779×10⁴ |
| .80000×10⁸ | .26307×10² | .24000×10⁹ | .14655×10⁴ | .40000×10⁹ | .74902×10⁴ |
| .10000×10⁹ | .65691×10² | .26000×10⁹ | .19025×10⁴ | .42000×10⁹ | .87235×10⁴ |
| .12000×10⁹ | .13219×10³ | .28000×10⁹ | .24174×10⁴ | .44000×10⁹ | .10084×10⁵ |
| .14000×10⁹ | .23248×10³ | .30000×10⁹ | .30165×10⁴ | .46000×10⁹ | .11578×10⁵ |
| .16000×10⁹ | .37307×10³ | .32000×10⁹ | .37060×10⁴ | .48000×10⁹ | .13211×10⁵ |
| .18000×10⁹ | .56035×10³ | .34000×10⁹ | .44919×10⁴ | .50000×10⁹ | .14990×10⁵ |
| log rho = 6.00 | | | | | |
| .40000×10⁸ | .80711×10⁰ | .20000×10⁹ | .15694×10⁴ | .36000×10⁹ | .11072×10⁵ |
| .60000×10⁸ | .98284×10¹ | .22000×10⁹ | .21800×10⁴ | .38000×10⁹ | .13161×10⁵ |
| .80000×10⁸ | .41696×10² | .24000×10⁹ | .29289×10⁴ | .40000×10⁹ | .15494×10⁵ |
| .10000×10⁹ | .11240×10³ | .26000×10⁹ | .38294×10⁴ | .42000×10⁹ | .18085×10⁵ |
| .12000×10⁹ | .23737×10³ | .28000×10⁹ | .48949×10⁴ | .44000×10⁹ | .20946×10⁵ |
| .14000×10⁹ | .43140×10³ | .30000×10⁹ | .61386×10⁴ | .46000×10⁹ | .24090×10⁵ |
| .16000×10⁹ | .70879×10³ | .32000×10⁹ | .75739×10⁴ | .48000×10⁹ | .27532×10⁵ |
| .18000×10⁹ | .10835×10⁴ | .34000×10⁹ | .92139×10⁴ | .50000×10⁹ | .31283×10⁵ |
| log rho = 6.20 | | | | | |
| .40000×10⁸ | .67726×10⁰ | .20000×10⁹ | .29029×10⁴ | .36000×10⁹ | .21789×10⁵ |
| .60000×10⁸ | .11768×10² | .22000×10⁹ | .40878×10⁴ | .38000×10⁹ | .25994×10⁵ |
| .80000×10⁸ | .59073×10² | .24000×10⁹ | .55529×10⁴ | .40000×10⁹ | .30699×10⁵ |
| .10000×10⁹ | .17521×10³ | .26000×10⁹ | .73263×10⁴ | .42000×10⁹ | .35933×10⁵ |
| .12000×10⁹ | .39311×10³ | .28000×10⁹ | .94360×10⁴ | .44000×10⁹ | .41722×10⁵ |
| .14000×10⁹ | .74457×10³ | .30000×10⁹ | .11910×10⁵ | .46000×10⁹ | .48094×10⁵ |
| .16000×10⁹ | .12603×10⁴ | .32000×10⁹ | .14775×10⁵ | .48000×10⁹ | .55075×10⁵ |
| .18000×10⁹ | .19700×10⁴ | .34000×10⁹ | .18059×10⁵ | .50000×10⁹ | .62693×10⁵ |

TABLE 1.—*Neutrino Emissivity by Transverse Plasmons—Continued*

| $T$ | $q$ sub $T$ | $T$ | $q$ sub $T$ | $T$ | $q$ sub $T$ |
|---|---|---|---|---|---|
| log rho = 6.40 | | | | | |
| .40000×10⁹ | .44834×10⁰ | .20000×10⁹ | .50338×10⁴ | .36000×10⁹ | .40850×10⁵ |
| .60000×10⁸ | .11950×10² | .22000×10⁹ | .72106×10⁴ | .38000×10⁹ | .48954×10⁵ |
| .80000×10⁸ | .73637×10² | .24000×10⁹ | .99315×10⁴ | .40000×10⁹ | 58048×10⁵ |
| .10000×10⁹ | .24563×10³ | .26000×10⁹ | .13254×10⁵ | .42000×10⁹ | .68187×10⁵ |
| .12000×10⁹ | .59398×10³ | .28000×10⁹ | .17234×10⁵ | .44000×10⁹ | .79425×10⁵ |
| .14000×10⁹ | .11843×10⁴ | .30000×10⁹ | .21928×10⁵ | .46000×10⁹ | .91817×10⁵ |
| .16000×10⁹ | .20801×10⁴ | .32000×10⁹ | .27392×10⁵ | .48000×10⁹ | .10901×10⁶ |
| .18000×10⁹ | .33433×10⁴ | .34000×10⁹ | .33681×10⁵ | .50000×10⁹ | .12028×10⁶ |
| log rho = 6.60 | | | | | |
| .40000×10⁸ | .22771×10⁰ | .20000×10⁹ | .81367×10⁴ | .36000×10⁹ | .72753×10⁵ |
| .60000×10⁸ | .10087×10² | .22000×10⁹ | .11905×10⁵ | .38000×10⁹ | .87684×10⁵ |
| .80000×10⁸ | .79523×10² | .24000×10⁹ | .16681×10⁵ | .40000×10⁹ | .10450×10⁶ |
| .10000×10⁹ | .30589×10³ | .26000×10⁹ | .22579×10⁵ | .42000×10⁹ | .12330×10⁶ |
| .12000×10⁹ | .81050×10³ | .28000×10⁹ | .29709×10⁵ | .44000×10⁹ | .14420×10⁶ |
| .14000×10⁹ | .17209×10⁴ | .30000×10⁹ | .38183×10⁵ | .46000×10⁹ | .16729×10⁶ |
| .16000×10⁹ | .31636×10⁴ | .32000×10⁹ | .48110×10⁵ | .48000×10⁹ | .19270×10⁶ |
| .18000×10⁹ | .52622×10⁴ | .34000×10⁹ | .59597×10⁵ | .50000×10⁹ | .22051×10⁶ |
| log rho = 6.80 | | | | | |
| .40000×10⁸ | .86165×10⁻¹ | .20000×10⁹ | .12199×10⁵ | .36000×10⁹ | .12289×10⁶ |
| .60000×10⁸ | .69370×10¹ | .22000×10⁹ | .18317×10⁵ | .38000×10⁹ | .14916×10⁶ |
| .80000×10⁸ | .73257×10² | .24000×10⁹ | .26213×10⁵ | .40000×10⁹ | .17887×10⁶ |
| .10000×10⁹ | .33420×10³ | .26000×10⁹ | .36104×10⁵ | .42000×10⁹ | .21225×10⁶ |
| .12000×10⁹ | .98873×10³ | .28000×10⁹ | .48205×10⁵ | .44000×10⁹ | .24944×10⁶ |
| .14000×10⁹ | .22657×10⁴ | .30000×10⁹ | .62727×10⁵ | .46000×10⁹ | .29069×10⁶ |
| .16000×10⁹ | .44028×10⁴ | .32000×10⁹ | .79878×10⁵ | .48000×10⁹ | .33618×10⁶ |
| .18000×10⁹ | .76364×10⁴ | .34000×10⁹ | .99864×10⁵ | .50000×10⁹ | .38611×10⁶ |
| log rho = 7.00 | | | | | |
| .40000×10⁸ | .23503×10⁻¹ | .20000×10⁹ | .16879×10⁵ | .36000×10⁹ | .17069×10⁶ |
| .60000×10⁸ | .38023×10¹ | .22000×10⁹ | .26157×10⁵ | .38000×10⁹ | .24081×10⁶ |
| .80000×10⁸ | .56626×10² | .24000×10⁹ | .38406×10⁵ | .40000×10⁹ | .29160×10⁶ |
| .10000×10⁹ | .31620×10³ | .26000×10⁹ | .54035×10⁵ | .42000×10⁹ | .34673×10⁶ |
| .12000×10⁹ | .10670×10⁴ | .28000×10⁹ | .73445×10⁵ | .44000×10⁹ | .41108×10⁶ |
| .14000×10⁹ | .26795×10⁴ | .30000×10⁹ | .97028×10⁵ | .46000×10⁹ | .48169×10⁶ |
| .16000×10⁹ | .55669×10⁴ | .32000×10⁹ | .12518×10⁶ | .48000×10⁹ | .55985×10⁶ |
| .18000×10⁹ | .10157×10⁵ | .34000×10⁹ | .15827×10⁶ | .50000×10⁹ | .64591×10⁶ |

TABLE 1.—*Neutrino Emissivity by Transverse Plasmons—Continued*

| $T$ | $q$ sub $T$ | $T$ | $q$ sub $T$ | $T$ | $q$ sub $T$ |
|---|---|---|---|---|---|
| log rho = 7.20 | | | | | |
| $.40000\times10^{8}$ | $.44441\times10^{-4}$ | $.20000\times10^{9}$ | $.21436\times10^{5}$ | $.36000\times10^{9}$ | $.29799\times10^{6}$ |
| $.60000\times10^{8}$ | $.16197\times10^{1}$ | $.22000\times10^{9}$ | $.34507\times10^{5}$ | $.38000\times10^{9}$ | $.36871\times10^{6}$ |
| $.80000\times10^{8}$ | $.36048\times10^{2}$ | $.24000\times10^{9}$ | $.52266\times10^{5}$ | $.40000\times10^{9}$ | $.44975\times10^{6}$ |
| $.10000\times10^{9}$ | $.25530\times10^{3}$ | $.26000\times10^{9}$ | $.75453\times10^{5}$ | $.42000\times10^{9}$ | $.54178\times10^{6}$ |
| $.12000\times10^{9}$ | $.10066\times10^{4}$ | $.28000\times10^{9}$ | $.10480\times10^{6}$ | $.44000\times10^{9}$ | $.64546\times10^{6}$ |
| $.14000\times10^{9}$ | $.28188\times10^{4}$ | $.30000\times10^{9}$ | $.14102\times10^{6}$ | $.46000\times10^{9}$ | $.76145\times10^{6}$ |
| $.16000\times10^{9}$ | $.63435\times10^{4}$ | $.32000\times10^{9}$ | $.18483\times10^{6}$ | $.48000\times10^{9}$ | $.89040\times10^{6}$ |
| $.18000\times10^{9}$ | $.12300\times10^{5}$ | $.34000\times10^{9}$ | $.23693\times10^{6}$ | $.50000\times10^{9}$ | $.10330\times10^{7}$ |
| log rho = 7.40 | | | | | |
| $.40000\times10^{8}$ | $.55558\times10^{-3}$ | $.20000\times10^{9}$ | $.24808\times10^{5}$ | $.36000\times10^{9}$ | $.42668\times10^{6}$ |
| $.60000\times10^{8}$ | $.52006\times10^{0}$ | $.22000\times10^{9}$ | $.41804\times10^{5}$ | $.38000\times10^{9}$ | $.53475\times10^{6}$ |
| $.80000\times10^{8}$ | $.18484\times10^{2}$ | $.24000\times10^{9}$ | $.65728\times10^{5}$ | $.40000\times10^{9}$ | $.65975\times10^{6}$ |
| $.10000\times10^{9}$ | $.17286\times10^{3}$ | $.26000\times10^{9}$ | $.97880\times10^{5}$ | $.42000\times10^{9}$ | $.80285\times10^{6}$ |
| $.12000\times10^{9}$ | $.81841\times10^{3}$ | $.28000\times10^{9}$ | $.13955\times10^{6}$ | $.44000\times10^{9}$ | $.96524\times10^{6}$ |
| $.14000\times10^{9}$ | $.26067\times10^{3}$ | $.30000\times10^{9}$ | $.19201\times10^{6}$ | $.46000\times10^{9}$ | $.11481\times10^{7}$ |
| $.16000\times10^{9}$ | $.64504\times10^{3}$ | $.32000\times10^{9}$ | $.25653\times10^{6}$ | $.48000\times10^{9}$ | $.13525\times10^{7}$ |
| $.18000\times10^{9}$ | $.13447\times10^{5}$ | $.34000\times10^{9}$ | $.33435\times10^{6}$ | $.50000\times10^{9}$ | $.15796\times10^{7}$ |
| log rho = 7.60 | | | | | |
| $.40000\times10^{8}$ | $.43345\times10^{-4}$ | $.20000\times10^{9}$ | $.25926\times10^{5}$ | $.36000\times10^{9}$ | $.57571\times10^{6}$ |
| $.60000\times10^{8}$ | $.12127\times10^{0}$ | $.22000\times10^{9}$ | $.46135\times10^{5}$ | $.38000\times10^{9}$ | $.73281\times10^{6}$ |
| $.80000\times10^{8}$ | $.74286\times10^{1}$ | $.24000\times10^{9}$ | $.75856\times10^{5}$ | $.40000\times10^{9}$ | $.91665\times10^{6}$ |
| $.10000\times10^{9}$ | $.96082\times10^{2}$ | $.26000\times10^{9}$ | $.11725\times10^{6}$ | $.42000\times10^{9}$ | $.11293\times10^{7}$ |
| $.12000\times10^{9}$ | $.56359\times10^{3}$ | $.28000\times10^{9}$ | $.17250\times10^{6}$ | $.44000\times10^{9}$ | $.13728\times10^{7}$ |
| $.14000\times10^{9}$ | $.20884\times10^{4}$ | $.30000\times10^{9}$ | $.24380\times10^{6}$ | $.46000\times10^{9}$ | $.16491\times10^{7}$ |
| $.16000\times10^{9}$ | $.57807\times10^{4}$ | $.32000\times10^{9}$ | $.33333\times10^{6}$ | $.48000\times10^{9}$ | $.19603\times10^{7}$ |
| $.18000\times10^{9}$ | $.13133\times10^{5}$ | $.34000\times10^{9}$ | $.44326\times10^{6}$ | $.50000\times10^{9}$ | $.23084\times10^{7}$ |
| log rho = 7.80 | | | | | |
| $.40000\times10^{8}$ | $.19678\times10^{-5}$ | $.20000\times10^{9}$ | $.24173\times10^{5}$ | $.36000\times10^{9}$ | $.72854\times10^{6}$ |
| $.60000\times10^{8}$ | $.19624\times10^{-1}$ | $.22000\times10^{9}$ | $.45895\times10^{5}$ | $.38000\times10^{9}$ | $.94488\times10^{6}$ |
| $.80000\times10^{8}$ | $.22635\times10^{1}$ | $.24000\times10^{9}$ | $.79592\times10^{5}$ | $.40000\times10^{9}$ | $.12017\times10^{7}$ |
| $.10000\times10^{9}$ | $.42712\times10^{2}$ | $.26000\times10^{9}$ | $.12862\times10^{6}$ | $.42000\times10^{9}$ | $.15027\times10^{7}$ |
| $.12000\times10^{9}$ | $.32175\times10^{3}$ | $.28000\times10^{9}$ | $.19648\times10^{6}$ | $.44000\times10^{9}$ | $.18513\times10^{7}$ |
| $.14000\times10^{9}$ | $.14235\times10^{4}$ | $.30000\times10^{9}$ | $.28677\times10^{6}$ | $.46000\times10^{9}$ | $.22509\times10^{7}$ |
| $.16000\times10^{9}$ | $.44951\times10^{4}$ | $.32000\times10^{9}$ | $.40311\times10^{6}$ | $.48000\times10^{9}$ | $.27051\times10^{7}$ |
| $.18000\times10^{9}$ | $.11302\times10^{5}$ | $.34000\times10^{9}$ | $.54916\times10^{6}$ | $.50000\times10^{9}$ | $.32172\times10^{7}$ |

TABLE 1.—*Neutrino Emissivity by Transverse Plasmons—Continued*

| $T$ | $q$ sub $T$ | $T$ | $q$ sub $T$ | $T$ | $q$ sub $T$ |
|---|---|---|---|---|---|
| log rho = 8.00 | | | | | |
| $.40000\times10^{8}$ | $.47800\times10^{-7}$ | $.20000\times10^{9}$ | $.19809\times10^{5}$ | $.36000\times10^{9}$ | $.85874\times10^{6}$ |
| $.60000\times10^{8}$ | $.20858\times10^{-2}$ | $.22000\times10^{9}$ | $.40604\times10^{5}$ | $.38000\times10^{9}$ | $.11391\times10^{7}$ |
| $.80000\times10^{8}$ | $.50212\times10^{0}$ | $.24000\times10^{9}$ | $.75007\times10^{5}$ | $.40000\times10^{9}$ | $.14781\times10^{7}$ |
| $.10000\times10^{9}$ | $.14708\times10^{2}$ | $.26000\times10^{9}$ | $.12779\times10^{6}$ | $.42000\times10^{9}$ | $.18817\times10^{7}$ |
| $.12000\times10^{9}$ | $.14833\times10^{3}$ | $.28000\times10^{9}$ | $.20417\times10^{6}$ | $.44000\times10^{9}$ | $.23558\times10^{7}$ |
| $.14000\times10^{9}$ | $.80734\times10^{3}$ | $.30000\times10^{9}$ | $.30965\times10^{6}$ | $.46000\times10^{9}$ | $.29063\times10^{7}$ |
| $.16000\times10^{9}$ | $.29750\times10^{4}$ | $.32000\times10^{9}$ | $.44998\times10^{6}$ | $.48000\times10^{9}$ | $.35392\times10^{7}$ |
| $.18000\times10^{9}$ | $.84264\times10^{4}$ | $.34000\times10^{9}$ | $.63103\times10^{6}$ | $.50000\times10^{9}$ | $.42601\times10^{7}$ |

# APPENDIX

## CALCULATION OF $x^3\mathfrak{F}(x)$ FOR SMALL $x$

Put $\eta = x\cosh\xi$ in equation (19); then

$$x^3\mathfrak{F}(x) = \int_x^\infty \frac{1}{e^\eta - 1}\left(1-\frac{x^2}{\eta^2}\right)^{1/2}\eta^2 d\eta. \tag{27}$$

By splitting the integral

$$x^3\mathfrak{F}(x) = \int_0^\infty \frac{1}{e^\eta-1}\eta^2 d\eta - \int_0^x \frac{\eta}{e^\eta-1}\eta d\eta - \frac{1}{2}x^2\int_x^\infty \frac{1}{e^\eta-1}d\eta + \int_x^\infty \frac{1}{e^\eta-1}\left[\left(1-\frac{x^2}{\eta^2}\right)^{1/2} - 1 + \frac{1}{2}\frac{x^2}{\eta^2}\right]\eta^2 d\eta,$$

or

$$x^3\mathfrak{F}(x) = 2\zeta(3) - a_1(x) + \tfrac{1}{2}x^2\ln(1-e^{-x}) + a_2(x). \tag{28}$$

Now

$$a_1(x) = \int_0^x\left[1-\frac{1}{2}\eta+\frac{1}{12}\eta^2-\frac{B_2}{4!}\eta^4+O(\eta^6)\right]\eta d\eta = \frac{1}{2}x^2-\frac{1}{6}x^3+\frac{1}{48}x^4-O(x^6) \tag{29}$$

for $x < 2\pi$.

An elementary calculation gives

$$\tfrac{1}{2}x^2\ln(1-e^{-x}) = \tfrac{1}{2}x^2\ln x - \tfrac{1}{4}x^3 + \tfrac{1}{48}x^4 - O(x^6). \tag{30}$$

The calculation of $a_2(x)$ is quite lengthy; we begin by splitting the integral again:

$$a_2(x) = -\frac{1}{8}x^4\int_A^\infty \frac{1}{e^\eta-1}\frac{d\eta}{\eta^2} + O(x^6) + \int_x^A \frac{1}{e^\eta-1}\left[\left(1-\frac{x^2}{\eta^2}\right)^{1/2} - 1 + \frac{1}{2}\frac{x^2}{\eta^2}\right]\eta^2 d\eta$$

$$= -\frac{1}{8}\left(\int_A^\infty \frac{1}{e^\eta-1}\frac{d\eta}{\eta^2}\right)x^4 + a_3(x) + O(x^6). \tag{31}$$

Put $n\xi = x$; then

$$(e^{\eta}-1)^{-1}\eta^2 d\eta = x^2\frac{x}{\xi}(e^{x/\xi}-1)^{-1}\frac{d\xi}{\xi^3}$$

and

$$a_3(x) = x^2\int_{x/A}^{1}\frac{x/\xi}{e^{x/\xi}-1}[(1-\xi^2)^{1/2}-1+\frac{1}{2}\xi^2]\frac{d\xi}{\xi^3} = x^2\int_{x/A}^{1}\left[1-\frac{1}{2}\frac{x}{\xi}+\frac{1}{12}\frac{x^2}{\xi^2}-\frac{B_2}{4!}\frac{x^4}{\xi^4}+\ldots+(-)^{n+1}\frac{B_n}{(2n)!}\frac{x^{2n}}{\xi^{2n}}\right.$$

$$\left.+\ldots\right]\cdot[(1-\xi^2)^{1/2}-1+\frac{1}{2}\xi^2]\frac{d\xi}{\xi^3},$$

where we require

$$\frac{x}{\xi}<2\pi \quad \text{or} \quad A<2\pi.$$

Integrating term by term, we get

$$a_3(x) = x^2 b_o(x)-\frac{1}{2}x^3 b_1(x)+\frac{1}{12}x^4 b_2(x)-\frac{B_2}{4!}x^6 b_4(x)+\ldots+(-)^{n+1}\frac{Bn}{(2n)!}x^{2n+2}b_{2n}(x)+\ldots, \tag{32}$$

where

$$b_m(x) = \int_{x/A}^{1}\left[(1-\xi^2)^{1/2}-1+\frac{1}{2}\xi^2\right]\frac{d\xi}{\xi^{3+m}}$$

These integrals are elementary; in particular

$$b_o(x) = \frac{1}{4}-\frac{1}{2}\ln 2+\frac{1}{16}(x/A)^2+O(x^4), \tag{33}$$

$$b_1(x) = -\frac{1}{6}+\frac{1}{8}\frac{x}{A}+O(x^3), \tag{34}$$

$$b_2(x) = \frac{1}{8}\ln\frac{x}{A}+\frac{1}{32}-\frac{1}{8}\ln 2+O(x^2), \tag{35}$$

$$b_4(x) = -\frac{1}{16}(x/A)^{-2}+O(\ln x); \tag{36}$$

and for $n>2$

$$b_{2n}(x) = -\frac{1}{8(2n-2)}\left(\frac{x}{A}\right)^{2-2n}+O(x^{4-2n}). \tag{37}$$

Substituting equations (33)–(37) into equation (32), we get

$$a_3(x) = \left(\frac{1}{4}-\frac{1}{2}\ln 2\right)x^2+\frac{1}{12}x^3+\frac{1}{96}x^4\ln x+\left[\frac{1}{16}\frac{1}{A^2}-\frac{1}{16}\frac{1}{A}-\frac{}{96}\ln A+\frac{1}{12}\left(\frac{1}{32}-\frac{1}{8}\ln 2\right)\right.$$

$$\left.+\frac{B_2}{4!\,16}A^2+\ldots+(-)^n\frac{B_n}{(2n)!\,8(2n-2)}A^{2n-2}+\ldots\right]x^4+O(x^6\ln x). \tag{38}$$

Substituting equations (29), (30), and (31) into equation (27), and using equation (38), we get

$$x^3\mathfrak{F}(x) = 2\zeta(3)+\frac{1}{2}x^2\ln x-\frac{1}{4}(2\ln 2+1)x^2+\frac{1}{96}x^4\ln x-\frac{1}{8}q(A)x^4+O(x^6\ln x), \tag{39}$$

re

$$q(A)=\int_A^\infty \frac{1}{e^\eta-1}\frac{d\eta}{\eta^2}-\frac{1}{2}\frac{1}{A^2}+\frac{1}{2}\frac{1}{A}+\frac{1}{12}\ln A+\frac{1}{12}\left(\ln 2-\frac{1}{4}\right)$$
$$-\frac{B_2}{4!\,2}A^2+\cdots+(-)^{n+1}\frac{B_n}{(2n)!\,(2n-2)}A^{2n-2}+\cdots, \tag{40}$$

$q(A)$ is, of course, a constant; it is, however, a bit difficult to evaluate. We will use the relations

$$\frac{1}{t}\frac{1}{e^t-1}+\frac{1}{2}\frac{1}{t}=\frac{1}{2t}\coth\frac{t}{2}=\sum_{n=1}^\infty\frac{2}{4n^2\pi^2+t^2}+\frac{1}{t^2}. \tag{41}$$

Using the first of equations (41) we find on integrating by parts

$$-\int_A^\infty \ln t\left[\frac{d}{dt}\left(\frac{1}{2t}\coth\frac{t}{2}-\frac{1}{t^2}\right)\right]dt=\int_A^\infty\frac{1}{e^t-1}\frac{dt}{t^2}-\frac{1}{2}\frac{1}{A^2}+1/(2A)+(1/12)\ln A+O(A^2\ln A)$$
$$\therefore\ q(A)=q(0)=-\int_0^\infty \ln t\left[\frac{d}{dt}\left(\frac{1}{2t}\coth\frac{t}{2}-\frac{1}{t^2}\right)\right]dt+\frac{\ln 2-\frac{1}{4}}{12}. \tag{42}$$

Substituting the second of equations (41) into equation (42), and using the absolute and uniform convergence of the series (Knopp 1963) we obtain

$$q(0)-\frac{1}{12}\left(\ln 2-\frac{1}{4}\right)=4\int_0^\infty t\ln t\left(\sum_{n=1}^\infty\frac{1}{(4n^2\pi^2+t^2)^2}\right)dt=4\sum_{n=1}^\infty B(2n\pi), \tag{43}$$

where

$$B(\xi)\equiv\int_0^\infty\frac{x\ln x}{(x^2+\xi^2)^2}dx.$$

Putting $x^2=y$, we get (deHaan 1963)

$$B(\xi)=\frac{1}{4}\int_0^\infty\frac{\ln y}{(\xi^2+\nu)^2}d\nu=\frac{1}{4}\frac{1}{\xi^2}\ln(\xi^2)=\frac{1}{2\xi^2}\ln\xi.$$

By using this in equation (43),

$$q(0)-\frac{1}{12}\left(\ln 2-\frac{1}{4}\right)=2\sum_{n=1}^\infty\frac{1}{(2n\pi)^2}\ln(2n\pi)=\frac{1}{2\pi^2}\left(\ln 2\pi\sum_{n=1}^\infty\frac{1}{n^2}+\sum_{n=1}^\infty\frac{\ln n}{n^2}\right). \tag{44}$$

But

$$\sum_{n=1}^\infty\left(\frac{1}{n^2}\right)=\zeta(2)=\frac{\pi^2}{6},$$

and

$$\sum_{n=1}^\infty\frac{\ln n}{n^2}=\left[-\frac{d}{dz}\sum_{n=1}^\infty e^{-z\ln n}\right]_{z=2}=-\zeta'(2).$$

So

$$q(0)=\frac{1}{12}\left(\ln 2-\frac{1}{4}+\ln 2\pi-\frac{\zeta'(2)}{\zeta(2)}\right). \tag{45}$$

Using this in equation (39)

$$x^3\mathfrak{F}(x)=2\zeta(3)+\frac{1}{2}x^2\ln x-\frac{1}{4}(2\ln 2+1)x^2+\frac{1}{96}x^4\ln x$$
$$-\frac{1}{96}\left(\ln 2-\frac{1}{4}+\ln 2\pi-\frac{\zeta'(2)}{\zeta(2)}\right)x^4+O(x^6\ln x). \tag{46}$$

## REFERENCES


ADAMS, B., RUDERMAN, M., and WOO, C. 1963, *Phys. Rev.* **129**, 1383.

Brookhaven. 1963, Brookhaven Conference on Fundamental Aspects of Weak Interactions, September, 1963 (to be published).

CHANDRASEKHAR, S. 1957, *Stellar Structure* (New York: Dover Publications), p. 398.

CHIU, H. -Y. 1961, *Phys. Rev.* **123**, 1040.

CHIU, H. -Y., and MORRISON, P. 1960, *Phys. Rev. Letters*, **5**, 573.

CHIU, H. -Y., and STABLER, R. 1961, *Phys. Rev.*, **122**, 1317.

GANDEL'MAN, G., and PINEAU, V. 1960, *Soviet Phys.—J.E.T.P.*, **10**, 764.

GREENWOOD, R. 1941, *Ann. Math.*, **42**, 778–805.

HAAN, B. DE. 1963, *Nouvelles Tables d'Intégrales Définies* (Hafner), p. 196.

HIEU, N. VAN, and SHABALIN, E. P. 1963, *Soviet Phys.—J.E.T.P.*, **17**, 681.

IDA, M., and VAHAKA, M., unpublished.

KNOPP, K. 1963, *Theory and Application of Infinite Series* (Hafner), p. 535.

MATINYAN, S., and TSILOSANI, N. 1962, *Soviet Phys.—J.E.T.P.*, **14**, 1195.

REEVES, H. 1963, *Ap. J.*, **138**, 79.

RITUS, V. 1962, *Soviet Phys.—J.E.T.P.*, **14**, 915.

ROSENBERG, L. 1963, *Phys. Rev.*, **129**, 2786.